Synthesis, characterisation and 3D-printing of responsive biodegradable polymers for regenerative medicine applications

MSc Thesis

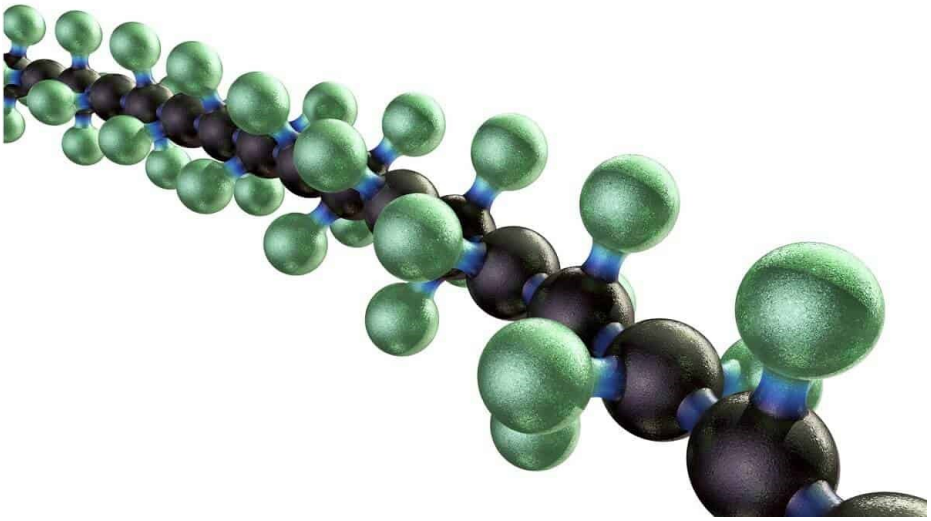

Myrto E. Vrentzou

MSc Program “Protein Biotechnology”

Department of Biology, University of Crete

Supervising Professor: Dr. Maria Vamvakaki

Supervising Faculty

Dr. Maria Vamvakaki, Professor, Department of Materials Science and Technology, University of Crete

Dr. Maria Chatzinikolaidou, Associate Professor, Department of Materials Science and Technology, University of Crete

Evaluation committee

Dr. Maria Vamvakaki, Professor, Department of Materials Science and Technology, University of Crete

Dr. Maria Chatzinikolaidou, Associate Professor, Department of Materials Science and Technology, University of Crete

Dr. Anna Mitraki, Professor, Department of Materials Science and Technology, University of Crete

Acknowledgements

I would like to thank Professor Maria Vamvakaki, for giving me the chance to work on a creative and demanding project and, despite my coming from an entirely different field, trusting me to learn an immense amount of new and interesting things pertaining to polymer synthesis and characterisation.

I would also like to thank Professor Maria Chatzinikolaidou, for her constant and enthusiastic support as co-supervisor of my thesis project, as well as her useful aid in the *in-vitro* and bioprinting-related experiments, and Professor Anna Mitraki, for graciously accepting to be a part of my evaluation committee.

No part of this project would have been possible without the calm and reassuring presence of Dr. Maria Kaliva, whose vast knowledge and guidance provided me with all the resources I needed to explore the fascinating world of polymers and biomaterials.

I am grateful to PhD candidate Mr. Konstantinos Loukelis for his cooperation and input regarding the bioprinting and biological evaluation experiments.

I must also express my heartfelt appreciation to Dr. Eva Vassilaki for her invaluable advice at numerous tricky parts of the project, as well as to Dr. Maria Psarrou and Dr. Theodore Manouras for their support.

Special thanks and a whole lot of love goes out to the members, current and former, of the Synthetic Materials Chemistry lab, for becoming a little everyday family for this entire year and a half. Marianna, George K., Anna, Dimitra, Rania, Dimitris F., Sofia, George P., Vassilis, Fernando, Theodora, Alex, Dimitris V., Jefta and Maria, I cannot thank you enough for all the lovely times we spent together in the lab.

Last, but certainly not least, I owe an incredibly large amount of gratitude to my family and friends for sticking by my side every step of the way. For the unending support, the encouragement to always do my best, the love.

Contents

Abbreviations

TE	**Tissue Engineering**
3D	**Three-dimensional**
ECM	**Extracellular Matrix**
-alt-	**Alternating copolymer**
LAP	**Laponite**
SEC	**Size Exclusion Chromatography**
GPC	**Gel Permeation Chromatography**
NMR	**Nuclear Magnetic Resonance**
UV	**Ultraviolet**
SEM	**Scanning Electron Microscopy**
THF	**Tetrahydrofuran**
TEA	**Triethylamine**
DCM	**Dichloromethane**
ADC	**Adipoyl Chloride**
TPAE	**Trimethylolpropane Allyl Ether**
DMF	**Dimethylformamide**
DMPA	**2,2-dimethoxy-2-phenylacetophenone**
PEGDMA	**poly(ethylene glycol) dimethacrylate**
EY	**Eosin Y**
TEOA	**Triethanolamine**
FBS	**Fetal Bovine Serum**

Abstract

Aliphatic polyesters comprise a group of richly diverse polymers with applications in many medical fields and tools, such as sutures, bone screws, drug delivery carrier systems and tissue engineering. These materials bear useful characteristics, such as enhanced biocompatibility and biodegradability. However, they are generally inert, without specific functionalities that would provide them with extra biological and responsive characteristics.

Thus, this thesis project focuses on the preparation of multifunctional pH-responsive biodegradable polyesters for tissue engineering applications. In particular, polyesters with carboxylic acid and alkene side groups were developed and studied. The carboxylic acid side groups provide pH-responsive properties and will enhance the hydrophilicity of the polyester, while the alkene side groups can be further used to covalently bind bioactive molecules and aid the formation of stable hydrogels.

The soft and rubbery texture of these polymer networks closely resembles that of a tissue's natural extracellular matrix. This makes them excellent candidates to be used as surrogate matrices for cell growth that more faithfully recapitulate the native, three-dimensional microenvironment of a cell, as opposed to the alterations in cell development driven by stiff, two-dimensional cell culture materials.

Therefore, the biodegradable, biocompatible, functional polyesters that were synthesised in this thesis project were tested and used as a bio-ink for the fabrication of cell-friendly, tissue engineering scaffolds. Extrusion-based additive manufacturing methods were employed for hydrogel printing, with the occasional addition of a nano-silicate clay (laponite) as rheology modifiers to improve texture and printability. The resulting scaffolds of different shapes and sizes were studied to determine swelling and porosity properties. Finally, the hydrogels were subjected to cell development and viability assays in a closely monitored cell culture environment.

1. Introduction

1.1. Tissue Engineering

Tissue engineering (TE) refers to a relatively new and highly interdisciplinary scientific field resting at the meeting point of biology, medicine, chemistry, materials science, physics, and engineering. Tissue failure due to traumatic injury, disease, developmental defects and senescence, combined with the constant need for transplantable tissue, has led to the emergence of the tissue engineering field to develop substitutes and constructs with the aim to maintain, enhance, restore or even replace native tissues (Katari et al., 2014).

This field aims at the creation of fully functional tissues, either partially or entirely stand-alone organs, bypassing the traditional risks and hurdles pertaining to organ transplant operations, namely biocompatibility, low biofunctionality, transplant rejection, graft-versus-host disease and other immunological complications. (Ikada et al., 2006)

That said, the generation of an at least functional tissue construct is no mean feat. A finely-tuned combination of cell culture techniques, scaffold fabrication, appropriate stimuli and growth factor delivery needs to be enforced. Cells are encouraged to grow in a predictable, directional way in order to synthesize a three-dimensional tissue sample, doing so on bioactive scaffolds that provide the cells with a friendly physicochemical environment and adequate support for controlled spatial growth. The process is often facilitated by the addition of growth factors and adhesion molecules, either as an external treatment, or as a built-in feature of the bioactive scaffold (adsorbed into the scaffold, or chemically bound into its basal structure) (Ding et al., 2021).

One of the first, crucial steps in the design and development of a tissue engineering construct is the choice of cells that will inhabit and grow inside the model. Cells of animal origin utilized in these experiments can be classified in three categories: *autologous* (cells extracted directly from the patient, with the intent of being re-inserted back into the same organism), *allogeneic* (derived from a donor, with the intent of being inserted into a different acceptor from the same species), and *xenogeneic* (derived from a donor, with the intent of being inserted into an acceptor of a different species) (Sávio-Silva et al., 2020). An obvious choice for a tissue engineering experiment would be the utilisation of cells of autologous origin, since they can

be highly effective and minimally, or not at all immunogenic. In a similar application, allogeneic and xenogeneic cell grafts could require additional immunosuppressive therapy in various degrees of intensity (Mastroianni et al., 2018). One major drawback in the usage of autologous cells would be harvesting them in sufficient quantities, which is immensely difficult in patients who are senior, or severely diseased and/or with significantly compromised cell-producing organs. The usage of autologous cell grafts is also not scalable, as it requires a case-to-case-tailored process of harvesting, assessing, culturing and re-introducing the cells to the patient (Osborn et al., 2020). Allogeneic cells have been notably used to treat conditions such as diabetes, hematopoietic organ deficiencies, cartilage deficiency or scarcity (for uses in plastic surgery) and dermal tissue conditions, such as extensive burns (Xu et al., 2021, Read-Fuller et al, 2018). Xenogeneic cells are not as frequently utilised as the other two categories, as their use is considered controversial, or even problematic at times, as it entails the danger of transmitting animal diseases to human tissue acceptors. As a proof, very few clinical trials are underway for the use of animal-derived xenogeneic grafts, and quite a few of them have failed in preliminary stages. Still, they are being used as transient solutions in organ transplantations, as a means for the native tissue to repair itself, or until a more suitable donor tissue is found. (El Masri et al., 2023)

Complementary, and of crucial importance to the selection of cells, is the existence of the necessary support for their growth. This is achieved by employing three-dimensional scaffolds that recapitulate the characteristics of the native extracellular matrix (ECM). These constructs have to abide by certain rules to facilitate cell viability, proliferation and differentiation. One of those rules is the existence of a pore network (Figure 1) that can aid in cell seeding and nutrient circulation and accessibility (Bružauskaitė et al., 2016).

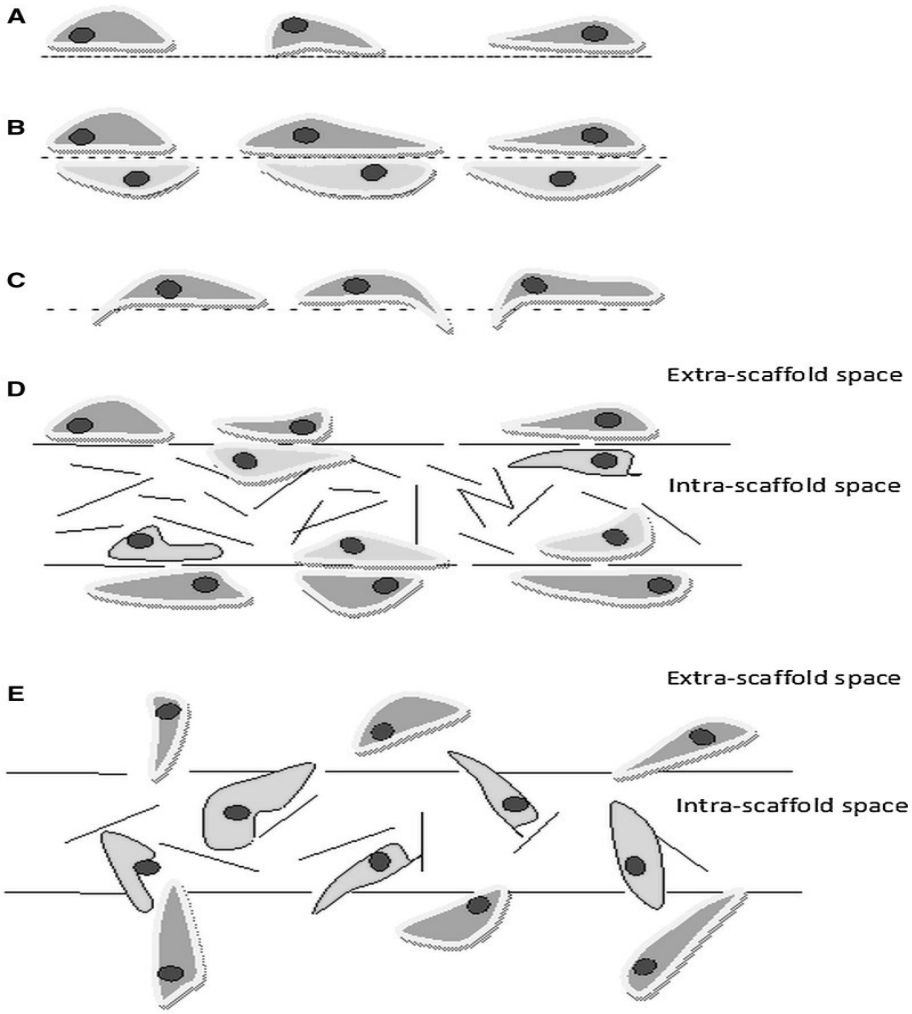

Figure 1. Selection of pore size for different applications: pore size ranging from <1μm to 1-3 μm to 3-12 μm for enhanced adhesion, anchorage-dependent cell-cell interaction and direct cell-cell contact in 2D hydrogels (a, b, c respectively), and pore size ranging from 1-3 μm to 100-800 μm for cell-cell interaction or free migration through 3D scaffolds (d, e respectively) (Bružauskaitė et al., 2016)

Furthermore, the mechanical properties of each scaffold should be in agreement with the requirements of each tissue engineering application (Figure 2). If the construct is being used to emulate or replace hard tissue, such as bone, then the degradation kinetics of the scaffold should allow for slow removal of material, so as to maintain adequate mechanical support while the ailing tissue regenerates. The opposite is true for soft tissue replacement, such as skin, where fast degradation of the scaffold makes for a more suitable tissue recovery.

Finally, material choice is also important in the development of scaffolds. The bioactive scaffolds can stem from compounds of natural origin (e.g. fibrin and collagen), synthetic ones (e.g. polyesters, ε-polycaprolactone, polyglycolide), inorganic powders and clays (e.g. β-tricalcium phosphate, bioactive glasses), as well as composite materials (e.g. carbon

nanotubules, graphene, etc.) (Bakhshandeh et al., 2017). Naturally, material choice heavily depends on the desired outcome, as it is the first point of contact of the cells with the scaffold, and thus a critical factor for adhesion and proliferation.

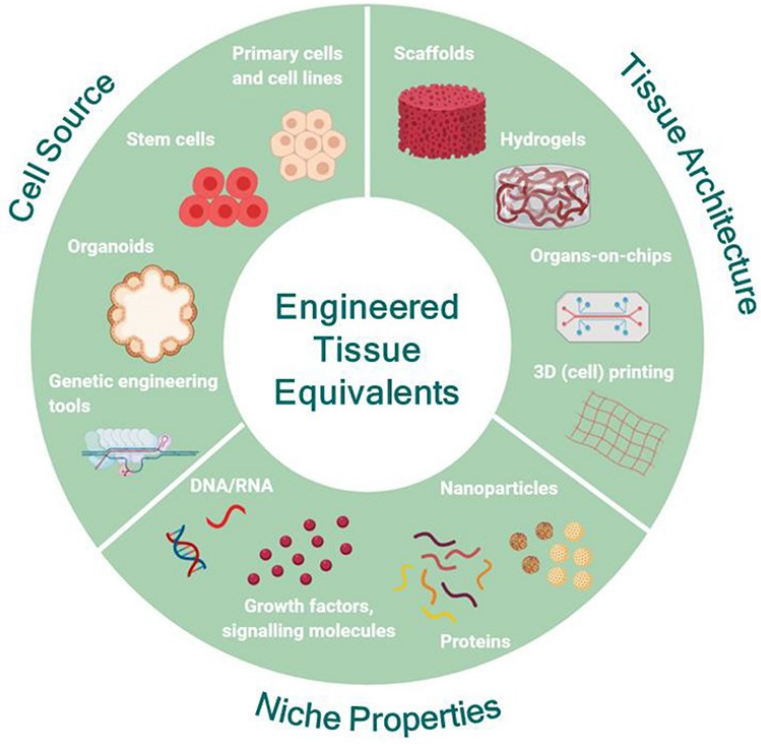

Figure 2. An overview of the main components of Tissue Engineering (Moysidou et al., 2021)

1.2. An Introduction to Polymers

1.2.1. Polymers and their Applications

Polymers is a field that has borne multiple innovative products of modern materials science and industry, ranging from plastics, clothing, surfaces and coatings, but also medicine, surgery, pharmaceuticals and drug delivery vehicles.

Polymers are entities of high molecular weight that are constituted by chains of repeating, covalently bound structural units (monomers). A polymer that only comprises one type of monomer repeat unit is called a *homopolymer,* whereas a polymer consisting of two or more

types of monomer repeat units is called a *copolymer (Figure 4).* These chains can also form more complex structures (Figure 3), held together through the formation of hydrogen bonds and dipole-dipole interactions.

1.2.2. Polymerisation Methods

Chain-growth or addition polymerisation: unsaturated monomer molecules get added onto the active site of a growing polymer chain one by one (Kricheldorf, 2009)

> *Free Radical Polymerisation*: successive addition of monomers at the end of a growing macro-radical results in the formation of a polymer chain
>
> *Cationic Polymerisation*: the reaction is initiated by an active cationic species
>
> *Anionic Polymerisation*: polymerisation is initiated by an active anionic species
>
> *Coordination Polymerisation*: this type of reaction is neither free radical nor ion-based. Instead, the monomers are attached to the growing chain in a strictly defined, stereoregular manner

Step-growth or condensation polymerisation: in this polymerisation species, bi-functional or multifunctional monomers first combine to form dimers. Then, the dimers can combine with each other, forming tetramers, or with single monomers to form trimers, then slightly longer oligomers, and finally, long polymer chains (Kricheldorf, 2009)

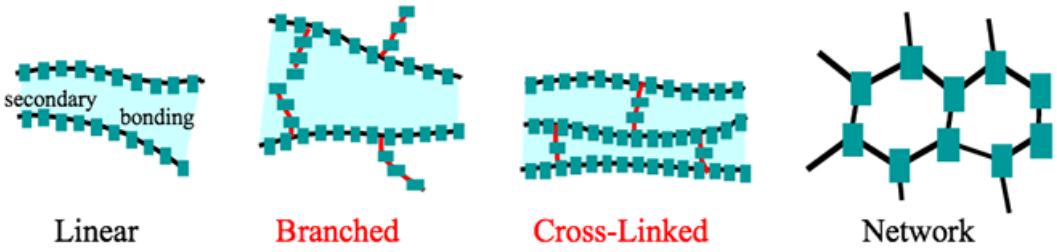

Figure 3: Types of polymer chain post-synthetic secondary bonding (Callister & Rethwisch 5e.)

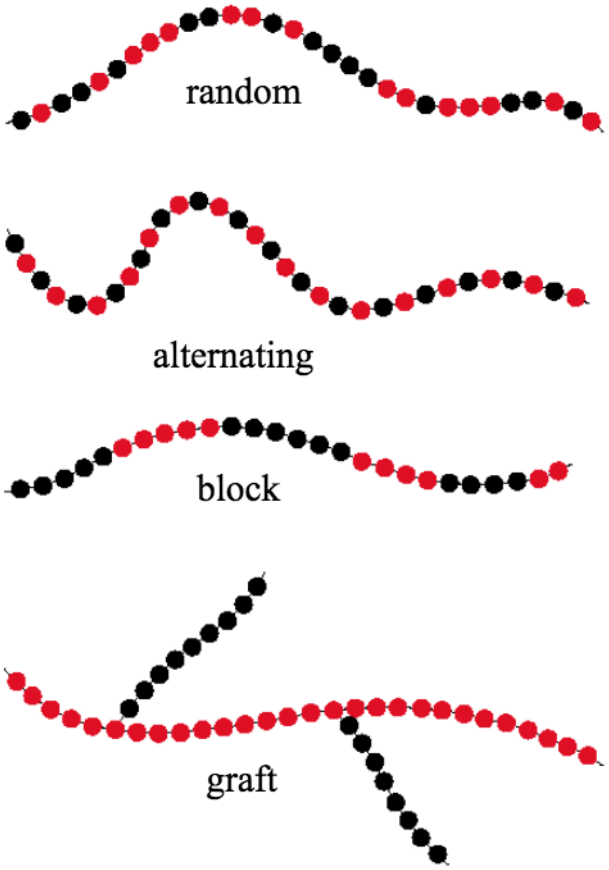

Figure 4. The four basic co-polymer structures (Callister &Rethwisch, 5e.)

1.2.3. Natural Polymers

Over the years, the tissue engineering field has constantly employed natural polymers, such as polypeptides, lipids and polysaccharides (Figure 5). Natural polymers possess an array of advantages, demonstrating increased biocompatibility, as well as bioactivity when present in tissue engineering scaffolds. They are relatively simple to isolate, both from mammalian (e.g. collagen, gelatin and elastin from bovine or porcine skin) and non-mammalian sources (e.g. alginate from brown seaweed, chitosan from the exoskeleton of crustaceans), making them adequately cheap and easily accessible, and they can quite faithfully emulate the natural extracellular matrix of cells (Guo et al., 2021). These polymers can function as 3D tissue scaffolds after being subjected to crosslinking reactions or by self-assembling, typically showcasing excellent cell growth and adhesion. Despite their attractively strong advantages,

natural polymers cannot guarantee fully reproducible results in scaffold fabrication due to varieties in their structure originating from their natural sources. The absence of impurities is an important factor that cannot be ascertained, propagating the risk of an unwarranted immune reaction. At the same time, their relatively poor mechanical properties and fast biodegradability are qualities that could render them poor candidates for 3D scaffold fabrication (Garg et al., 2011).

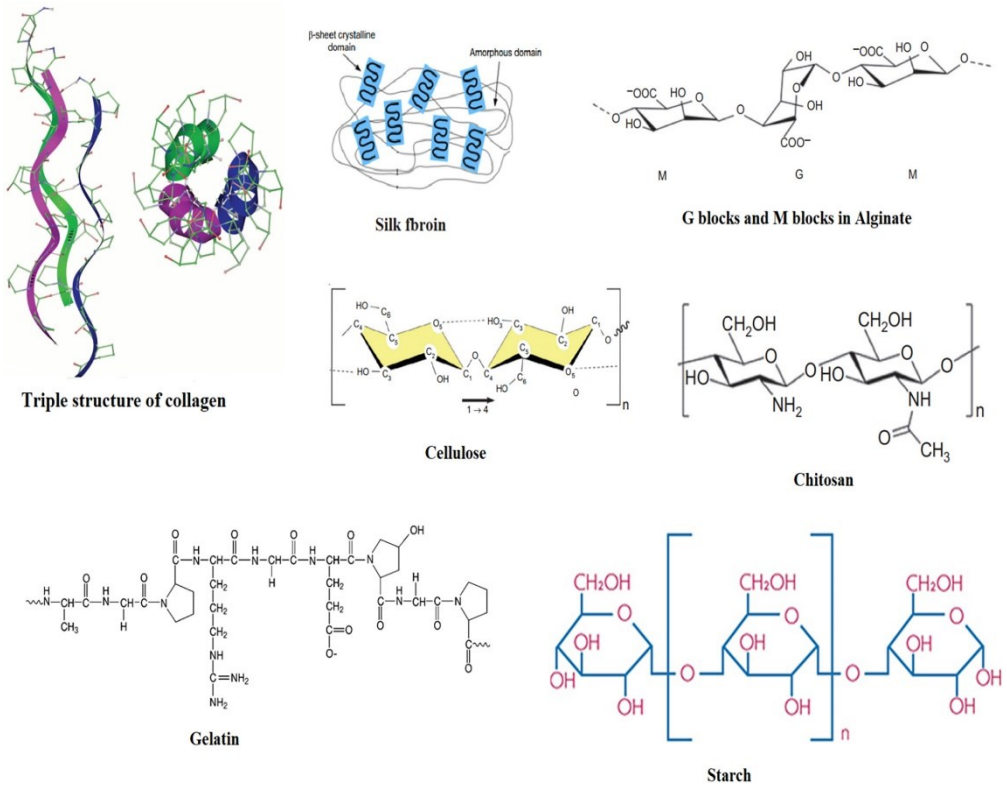

Figure 5. Common natural polymers used in biomedical applications, and their basic structures (Guo et al., 2021)

1.2.4. Synthetic Polymers

In order to overcome the various shortcomings of natural polymers, synthetic polymers have been designed to bridge the gap between bioactivity, cell-friendliness and mechanical properties. In 3D scaffold design, where natural polymers typically fail (limited reproducibility, impurities and unpredictable mechanical properties), synthetic polymers can be tailor-made with distinct architectures, chemical and mechanical properties to fabricate sturdy and often tunable or responsive 3D scaffolds. Amongst the most widely-used synthetic polymers are

polylactic acid (PLA, widely used in additive manufacturing), poly(ε-caprolactone) (PCL) and poly(ethylene glycol) (PEG). These polymers are biocompatible, biodegradable and quite a few of them are FDA-approved and have been assimilated into clinical practice. Initially, the use of these materials was limited to the fabrication of expendable materials, such as sutures, but with time, their use has been broadened to vaccine making and drug delivery, as well as in the tissue engineering field. (Kohane and Langer, 2008) However, just as with natural polymers, the various advantages of synthetic polymers also entail a number of drawbacks, the most notable of which being the relative scarcity of adhesion foci, as well as the potential generation of cytotoxic products during scaffold degradation. (Reddy et al., 2021)

1.2.5. Responsive Polymers

A major part of modern polymerisation reactions aim to synthesize stimuli-responsive ("smart") polymers. The stimuli (Figure 6) can be either natural (temperature, electromagnetic field), mechanical or chemical (pH), and can result in, mostly reversible, changes in the polymer chain structure, chain-chain or chain-solvent interactions. Some stimuli can act on a more macroscopic level, affecting intermolecular interactions by altering the thermodynamic parameters such as entropy. (Wei et al, 2017, Kim et al, 2017)

The most commonly known responsive polymers are:

- Temperature-responsive polymers: These polymers undergo changes in their solubility or swelling behavior in response to temperature variations. A well-known example is poly(N-isopropylacrylamide) (PNIPAAm), which exhibits a lower critical solution temperature (LCST) around 32 °C. Below this temperature, it is highly soluble in water, but above it, it becomes hydrophobic and precipitates out of solution. Applications of temperature-responsive polymers include their use in drug delivery, smart textiles, and tissue engineering (Doberenz et al., 2020).
- pH-responsive polymers: These polymers change their structure or solubility in response to changes in the solution pH. For example, poly(acrylic acid) (PAA) becomes increasingly soluble in water as the pH increases, due to the deprotonation of the carboxylic acid groups. pH-responsive polymers find applications in drug delivery, sensors, and controlled release systems (Kocak et al., 2017).

- Light-responsive polymers: These polymers undergo structural changes in response to light, typically ultraviolet (UV) or visible light. Azobenzene-based polymers are a common example, as they can undergo reversible photoisomerization between the trans and cis forms upon light irradiation. These polymers are used in optical devices, surface patterning, and drug delivery (Stoychev et al., 2019).
- Electrically-responsive polymers: Also known as electroactive polymers, these materials change their shape, size, or other properties in response to an applied electric field. Examples include polyaniline and polypyrrole. They are used in actuators, sensors, artificial muscles, and electrochromic devices, and could also be utilized in the controlled, pulsatile release of immobilised or encapsulated pharmaceutical products from drug delivery systems (Sénéchal et al., 2017).
- Magnetic-responsive polymers: These polymers contain magnetic particles or domains that respond to an external magnetic field by changing their shape, alignment, or other properties. Applications include drug delivery systems, separation techniques, and tissue engineering (Thevenot et al., 2013).

The design of carriers and polymeric structures with responsive polymers is an important pursuit in modern medicine, as they can be used to better target drugs and improve their specificity and release profile, aiming them towards ailing areas in which a certain stimulus is present (for example, acidic conditions in tumor or osteoclast microenvironments, or temperature increase in inflamed areas). These carriers will comprise a formidable alternative to currently used liposomes, which are generally biocompatible, albeit physicochemically unstable and sensitive to degradation (Gu et al, 2017, Karanth et al, 2007). The use of these liposomal structures is now beginning to be substituted, or also complemented by polymeric micelles, which have the capacity of hosting both hydrophobic and hydrophilic drugs in their hydrophobic core and hydrophilic corona, respectively. (Schmaljohann et al, 2006)

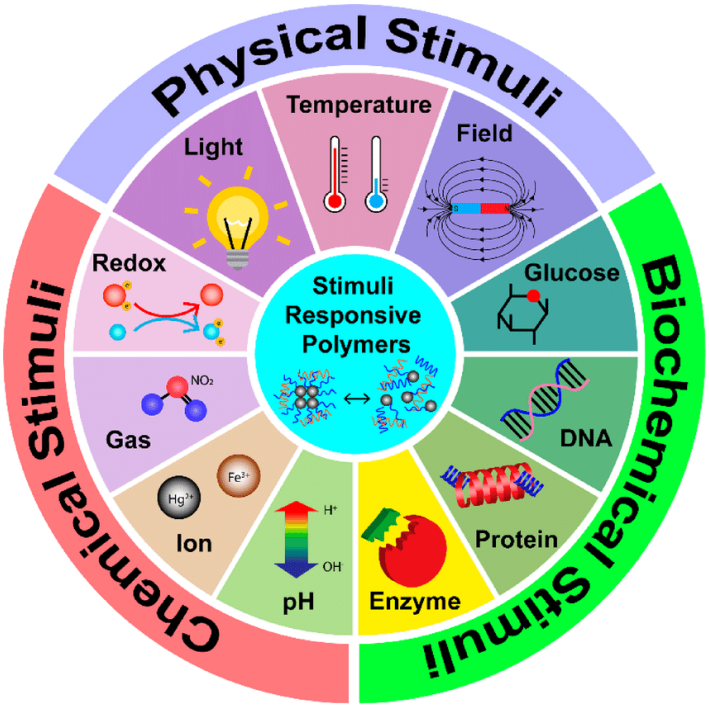

Figure 6. Types of stimuli that can change the structure of responsive polymers (Sun et al., 2020)

1.3. Composite Materials

As would be expected, none of the aforementioned types of biomaterials come without their respective disadvantages. Thus, combining two or more different biomaterials with distinctly different properties (e.g. synthetic polymers with inorganic fillers, such as various nanoclays, or synthetic and natural polymers), could result in a composite material that can combine the desirable properties of the two, while mitigating their shortcomings to create a scaffold that is unique and adapted to each individual purpose and application. (Aslam Khan et al., 2021) Key considerations for employing composite materials are the following:

- Biocompatibility: Composite materials used in tissue engineering can offer enhanced biocompatibility, aiding in the avoidance of an unwanted immune response when implanted into the body. This property ensures that the material does not cause harm to the surrounding tissues and cells. (Schmalz and Galler, 2017)
- Mechanical Properties: Tissues in the human body have varying mechanical properties depending on their function. Composite materials can be engineered to mimic these

properties, providing mechanical support to the engineered tissue and promoting proper function.

- Structural Support: Composite materials often serve as scaffolds or matrices that provide structural support for cell growth and tissue regeneration. These scaffolds mimic the natural extracellular matrix (ECM) and provide a framework for cells to adhere, proliferate, and differentiate.
- Bioactivity: Composite materials can be designed to have bioactive properties, such as the ability to promote cell adhesion, proliferation, and differentiation. This can be achieved by incorporating bioactive molecules, such as growth factors or peptides, into the composite matrix.
- Degradation Kinetics: The degradation kinetics of composite materials are important for tissue engineering applications. Ideally, the material should degrade at a rate that matches the rate of tissue regeneration, allowing the engineered tissue to gradually replace the scaffold over time. (Boccaccini et al., 2005)
- Electrical and Thermal Properties: In some tissue engineering applications, particularly those involving nerve or muscle regeneration, composite materials with specific electrical or thermal properties may be required to promote cell function and integration with native tissues. (Acharya et al., 2023)
- Nanocomposites: Nanocomposite materials, which incorporate nanoscale components such as nanoparticles, nanofibers and nanoclays, have shown promise in tissue engineering due to their unique mechanical, electrical, and biological properties. These materials can also enhance cell adhesion, proliferation, and differentiation, leading to improved tissue regeneration outcomes. (Armentano et al., 2010)

1.4. Aliphatic Polyesters in Tissue Engineering

Aliphatic polyesters rank highly among the frequently used biodegradable polymers in biomedical applications and thus have been extensively studied. Given the prevalence of ester linkages in nature, it is reasonable to anticipate that synthetic polymers containing such bonds as well as a similar structure would display degradable characteristics. Polyesters are able to form stable, porous materials that either do not degrade while in the form of scaffolds for

tissue culture, or they do so in a slow, controlled, and sometimes tunable manner (BaoLin and Ma, 2014). This is especially important, as it is possible to take advantage of the material's degradation rate to administer therapeutic molecules. (Casalini, 2017)

Indeed, well-known aliphatic polyesters such as the aforementioned PLA and PCL have been utilised in numerous applications as biodegradable biomaterials in drug delivery and tissue engineering due to their ability to break down under the influence of various cells and tissue microenvironments. The degradation of aliphatic polyesters primarily occurs through the hydrolysis of main chain ester linkages, and the rate and extent of degradation depend on the polymer properties such as hydrophilicity and crystallinity, while degradation can occur through bulk or surface erosion. (von Burkersroda et al., 2002)

Despite their notable characteristics, polyesters have certain drawbacks, the most prominent being their hydrophobic nature and the absence of functional pendant groups along the polymer backbone. Functional pendant groups, such as amines, hydroxyls, and carboxylic acids, can modify the physicochemical and biological properties of a biomaterial, impacting cellular adhesion, growth, and differentiation on biomaterial scaffolds. Additionally, cellular activity can be influenced by attaching bioactive compounds, such as proteins and peptides, onto the polymer, additions that are greatly facilitated by the existence of functional pendant groups. Lastly, incorporating stimuli-responsive functional groups (e.g., pH, temperature, light) can impart extraordinary properties and adjustable behavior to polymers. Thus, it is evident that the development of materials with these properties can enhance the landscape of the tissue engineering field. (Vignolini and Bruns, 2018)

1.5 Polycondensation Reactions

A large sub-category of synthetic polymeric materials is formed via condensation polymerisation reactions, as opposed to chain-growth reactions. Here, the reaction takes place through the transformation of the functional groups of the reactants, without the involvement of reactive species such as radicals. In this reaction type, a fusion of two monomers normally results in the loss of a byproduct, typically water or a hydrogenated molecule, and the end-product tends to have an *alternating* bonding pattern (Figure7).

Instead of C-C bond formation, typically characteristic of chain-growth reactions, the main type of bonding in step-growth polymerisation occurs between carbon and a heteroatom.

Polycondensation reactions tend to require more time to proceed than addition reactions, and generally yield products of lower molecular weight. The functional groups at the ends of each chain remain available for bonding, thus chains of shorter length can combine into longer ones towards the end of the reaction. The chains can interact post-synthesis if polar functional atoms are present, often leading to crystalline structures. (Reusch, 2010)

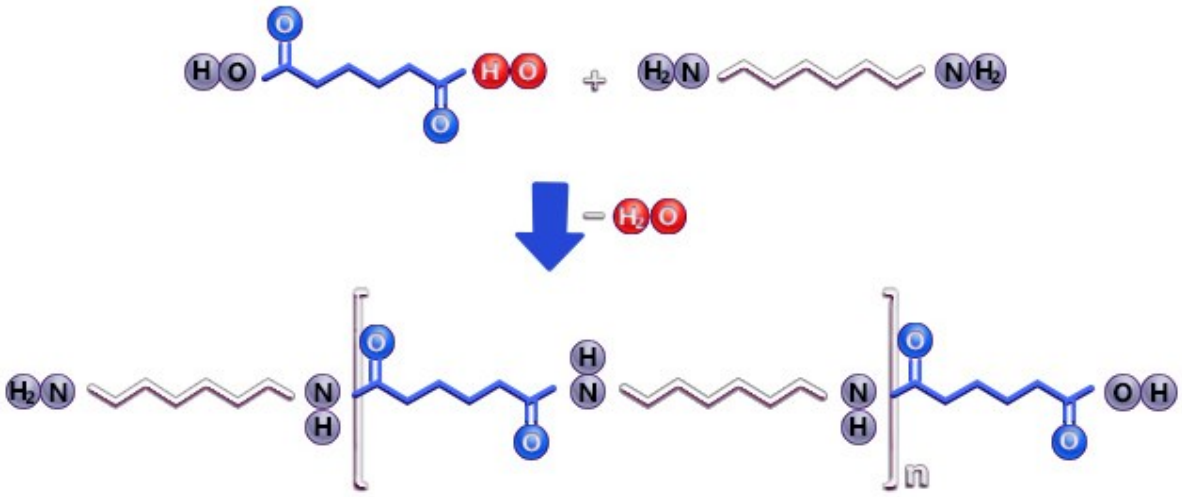

Figure 7. Polyesters and polyamines (pictured above) are polymers typically yielded by polycondensation reactions. (©PLEXPERT)

1.6. 3D Printing and Bio-printing

Additive manufacturing encompasses a range of techniques used to create objects by depositing a material layer by layer, as opposed to traditional subtractive methods.

3D printing is an additive manufacturing technique established in the early 1980s and, until today, it has experienced extraordinary advances, marking saltatory progress in various

applications, such as construction, industrial design, tool manufacturing, as well as in the health sector (Khorsandi et al., 2021).

Conventional 3D printing, a subset of additive manufacturing, employs various materials such as plastics, metals, and ceramics to produce objects with precise geometries. Techniques like fused deposition modelling (FDM), stereolithography (SLA), and selective laser sintering (SLS) are commonly utilized in industries ranging from aerospace to consumer goods (Figure 8).

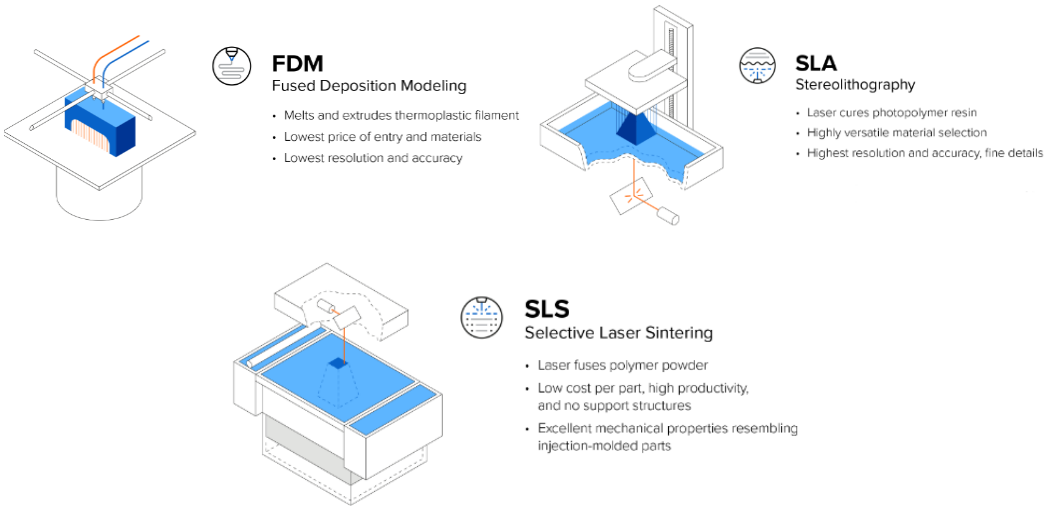

Figure 8. Common methods of additive manufacturing: Fused Deposition Modeling (FDM), Stereolithography (SLA) and Selective Laser Sintering (SLS) (©Formlabs)

In contrast to conventional 3D printing, 3D bioprinting focuses on fabricating living tissues and organs using bioinks composed of cells, growth factors, and biomaterials, making use of a vast array of different material deposition and construct fabrication techniques (Figure 9). In the ever-evolving landscape of medical technology, 3D bioprinting stands out as a revolutionary approach with the potential to transform the field of regenerative medicine. At its core, 3D bioprinting leverages the principles of additive manufacturing to fabricate intricate three-dimensional structures from biological materials, also called “bioinks”. This technology holds immense promise for regenerative medicine, offering the potential to address organ shortage crises and revolutionize personalized medicine.

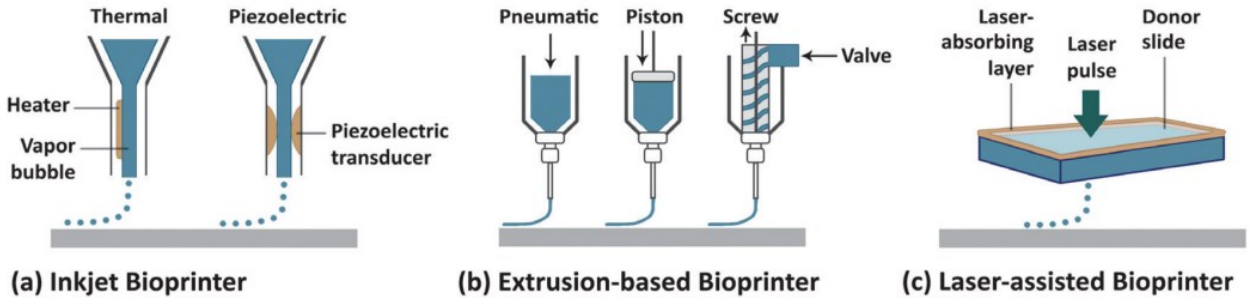

Figure 9. Types of scaffold preparation in 3D Bioprinting (Gungor-Ozkerim et al., 2018)

Bioprinting inks, or "bioinks" can fall under several categories, depending on their purity, content and applications. Three major types that these inks are the hydrogel-based, cell aggregate or pellet-based, and composite or bioactive molecule laden bioinks. This categorisation is largely notional, and does not exclude the possibility of a bioink pertaining to two categories at once (e.g. a bioink can be both hydrogel-based, as well as a composite material)

Cell aggregate-based bioinks are a type of bioink used in 3D bioprinting that incorporate pre-formed aggregates of cells into a biomaterial matrix. These aggregates, also known as spheroids or cellular aggregates, are typically composed of cells that have self-assembled into spherical structures through cell-cell interactions. In cell aggregate-based bioinks, the cell aggregates are suspended within a biocompatible matrix, providing structural support and facilitating their deposition during the bioprinting process. Composite bioinks are bioink formulations that incorporate multiple components, such as cells, biomaterials, growth factors, and bioactive molecules, to enhance the mechanical properties, bioactivity, and functionality of the printed constructs. By combining different materials with complementary properties, composite bioinks can overcome the limitations of individual components and tailor the properties of the printed tissue to specific applications. They often consist of a combination of natural and synthetic polymers, such as alginate, gelatin, hyaluronic acid, polyethylene glycol (PEG), or polycaprolactone (PCL), blended with cells and bioactive factors. These components can be mixed in various ratios and concentrations to achieve the desired viscosity, printability, and biological performance. (Gungor-Ozkerim et al., 2018)

Hydrogel-based bioinks, which are the centerpiece of this study, are water-containing polymer networks that are formed by crosslinked polymer chains. Due to the softness of their texture, their high water absorption and retention capacity, as well as their porosity, they are widely regarded as suitable and versatile materials for numerous biomedical applications (Figure 10), including the emulation of soft and hard living tissue microenvironments (Ho et al., 2022). Key considerations for a hydrogel to be eligible for use as a bioink are the following:

- The hydrogel should exhibit appropriate rheological properties, such as viscosity, shear-thinning behavior, and gelation kinetics, to enable extrusion-based bioprinting processes. These properties ensure that the bioink can be accurately deposited and maintain its structural integrity during printing.
- Hydrogel bioinks should support high cell viability and maintain cell functionality throughout the bioprinting process and during subsequent culture. The hydrogel matrix should provide a supportive microenvironment for cells, promoting cell adhesion, proliferation, and differentiation within the printed construct.
- The hydrogel should be biodegradable and, if possible, controllably so. Biodegradable hydrogel bioinks degrade over time, allowing for the remodeling and integration of the printed tissue construct into the surrounding tissue environment. This property is crucial for tissue regeneration and remodeling processes *in vivo*, as it facilitates the replacement of the hydrogel scaffold with native extracellular matrix components produced by cells.

In recent years, many polymer networks have been developed into “smart” hydrogels which, as previously mentioned, are able to respond to various stimuli, such as temperature, pH magnetic field, etc, thus changing their water content, structure and cell adhesion properties.

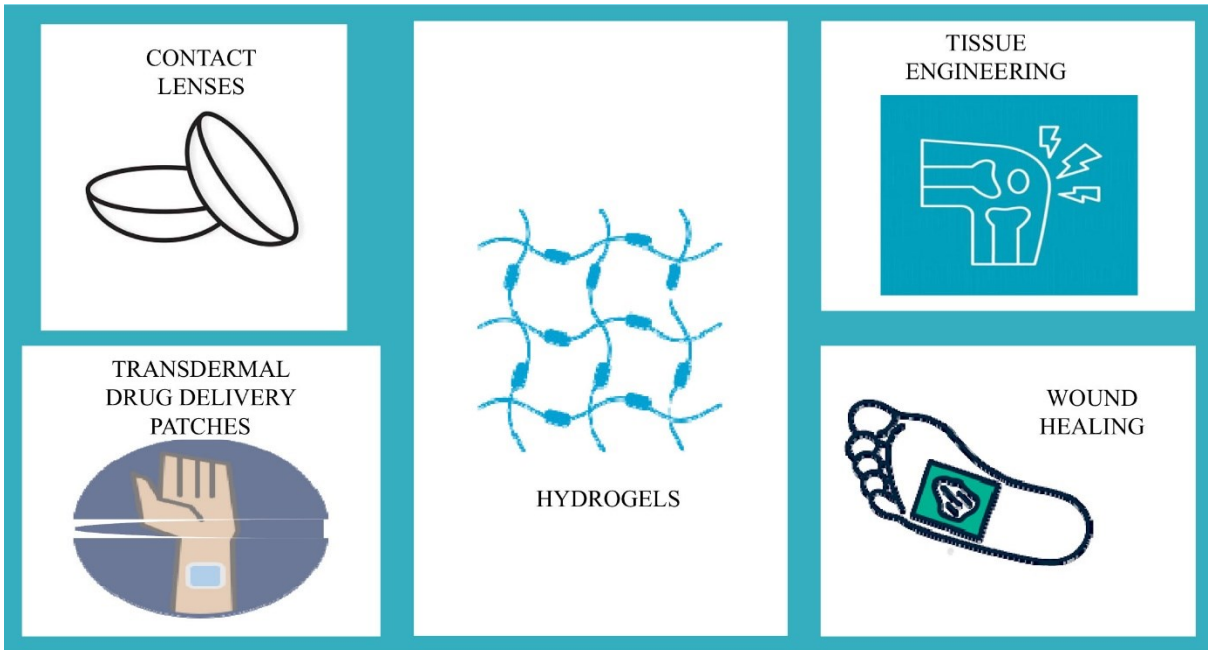

Figure 10. Biomedical applications of hydrogels (Chopra et al., 2022)

1.7. Aim of this Project

This work aimed to modify the aliphatic, alternating copolymer poly(TPAE-*alt*-AD), created by the condensation reaction of trimethylolpropane allyl ether (TPAE) with adipoyl chloride (AD), and document the synthesis of a extrusible, and later 3D-printable, hydrogel-based cell-laden bioink.

As documented in previous work from this laboratory, the polymer poly(TPAE-*alt*-AD) is hydrophobic and inert, thus further modification is necessary to alter its properties and render it suitable for use as a cell growth substrate. This was done by introducing a mercaptocarboxylic compound, thioglycolic acid, and binding it to the polymer via a UV-mediated, thiol-ene free radical "click" reaction. This process, also known as alkene hydrothiolation, takes place between an alkene ($H_2C=CH_2$) and a thiol (R-SH) to form a thioether (R-S-R'). The reaction, depending on the quantities of the reagents involved, as well as the irradiation time, can result in exceptional temporal control of the degree of functionalisation. The resulting product is a pH-responsive, hydrophilic polyester that can be used as an appropriate material for cell scaffold fabrication.

Next, the modified polymer was pre-crosslinked and extruded using a 3D printer to fabricate cell scaffolds. For that to become possible, cell-friendly cross-linking systems had to be tested and optimized. These approaches are presented and reported in this thesis.

Below the polymer (p[TPAE-alt-AD]) is referred to as simply PE (polyester), and when substituted by thioglycolic acid at certain modification degree, it is referred to as PE-GlycX, where "X" is the degree of functionalisation.

2. Experimental Part

2.1. Materials

Trimethylolpropane allyl ether (98%), adipoyl chloride (98%), pyridine (99.5%), thioglycolic acid (98%), 2,2-dimethoxy-2-phenyl-acetophenone (99%), chloroform (≥99.8%), methanol (≥99.8%), dimethylformamide (≥99.8%), Eosin Y Disodium Salt (≥85%) and Triethanolamine (≥99%) were purchased from Sigma-Aldrich (Steinheim, Germany). Tetrahydrofuran (THF, ≥99.8%) was purchased from Fisher Scientific (Geel, Belgium). Dichloromethane (analytical grade), n-hexane (96%), and diethyl ether (99.8%) were purchased from Scharlau (Sentmenat, Spain).

Trypsin/EDTA (0.25%), phosphate buffer saline, Amphotericin-B (fungizone), penicillin/streptomycin (P/S), were all purchased from Gibco ThermoFisher Scientific (Waltham, MA, USA), alpha-MEM cell culture medium and fetal bovine serum from PAN-Biotech (Aidenbach, Germany) and MC3T3-E1 pre-osteoblastic cells isolated from newborn mouse calvaria were purchased from DSMZ (Braunschweig, Germany). The live/dead cell viability assay kit was purchased from Biotium (Fremont, CA, USA).

2.2. Synthesis of poly[TPAE-alt-AD]

10 ml of Trimethylolpropane allyl ether (TPAE) were dissolved in 120 ml of dry dichloromethane (DCM, stirred overnight with calcium hydride, allowed to sit and then passed through a syringe filter). The solution was degassed with nitrogen gas for 20 min in an ice bath. 10.31 ml of dry, anhydrous pyridine were added to the reaction mixture as a HCl scavenger. Then, adipoyl chloride (ADC, distilled and degassed) was added dropwise to the solution. The reaction was left to proceed for 67 h at room temperature.

To obtain the product, the reaction flask was opened and the mixture was filtered to remove the salt formed by pyridine and HCl. The filtrate was evaporated and left to precipitate in cold methanol for about two days. After the end of this process, the excess methanol was discarded and the product was dried overnight in a vacuum oven.

^{1}H NMR (500 MHz, $CDCl_3$): δ 5.77–5.90 ppm (m, CH_2=CH–), δ 5.12–5.27 ppm (m, CH_2=CH–), δ 4.01 (s, –C(O)OCH_2–), δ 3.90–3.93 ppm (m, – OCH_2CH=CH2), δ 3.29 ppm (s, –CH_2OCH_2–), δ 2.30–2.34 ppm (t, –O(O)CCH_2–), δ 1.61– 1.66 ppm (m, –O(O)CCH_2CH_2–), δ 1.40–1.49 ppm (q, –CH_2CH_3), δ 0.83–0.88 ppm (t, – CH_2CH_3).

2.3. Synthesis of functional polyesters with carboxylic acid side groups

1 gr of poly[TPAE-*alt*-AD] was dissolved in 4 ml of N,N-dimethylformamide (DMF) and the solution was introduced in a 50 ml round-bottom Schott-Duran flask wrapped in aluminium foil. 180 mg of 2,2-dimethoxy-2-phenylacetophenone (DMPA) was added to the solution as a UV-activated, free radical photoinitiator. 367 μl of thioglycolic acid were introduced to the reaction mixture and stirred under a nitrogen atmosphere for 6 min. The reaction mixture was then uncovered and irradiated with UV light (λ = 365 nm) for a certain amount of time, until a degree of functionalisation of 80% was achieved. This degree of functionalization was chosen due to its enhanced biocompatibility with fibroblast cells when used in thin films (Mountaki et al., 2021).

To obtain the product, the reaction solution was introduced in a semipermeable membrane and dialysed against methanol for 24 h to remove the unreacted thioglycolic acid, DMPA and DMF. However, given the fact that these membranes tend to dry up, harden and their contents become difficult to access in the presence of methanol, traditional dialysis was not successful. Instead, overnight methanol precipitation was preferred. In a pinch, precipitation in a mixture of equal parts of n-hexane and diethyl ether (Hex/Eth) can be performed. This yields a defined product layer almost instantly, though at the cost of an increased presence of impurities (Figure).

^{1}H NMR (300 MHz, acetone–d6) for PE-Glyc100: : δ 4.02 ppm (s, –C(O)OCH_2–) δ 3.48–3.52 ppm (t, – OCH_2CH_2–), δ 3.36 ppm (s, –CCH_2O–), δ 3.25 ppm (s, –(O)CCH_2S–), δ 2.69–2.74 ppm (t, – CH_2CH_2S–), δ 2.37 ppm (s, –O(O)CCH_2–), δ 1.80–1.89 ppm (m, –$OCH_2CH_2CH_2S$–),), δ 1.64 ppm(s, –O(O)CCH_2CH_2–), δ 1.43–1.50 ppm (q, –CH_2CH_3), δ 0.86–0.91 ppm (t, –CH_2CH_3).

Quantification of the reaction yield (degree of functionalisation) was determined through the relative peak intensities of the NMR spectrum of the product. The integral of the protons of group “a” were normalised to 300 (three protons in the group, multiplied by 100) and then the integrals of protons “h” and “i” (one and two, respectively, on each side of the double bond) were calculated to find the degree of functionalisation.

2.4. Synthesis of gelatin merthacrylamide (GelMA)

The synthesis of gelatin methacrylamide was carried out according to a method reported by Parkatzidis et al. In a round-bottom flask, 2 g of Type B Gelatin were dissolved in PBS at 50 °C to form a 10% w/w solution. 0.8 mL of methacrylic anhydride (MAA) were introduced to the flask to achieve a gelatin/MAA ratio of 1:0.4, and stirred at 50 °C for one h. The reaction mixture was then rapidly precipitated in an 8-fold volume of acetonitrile. The supernatant was discarded and the product was allowed to air-dry slightly (to remove excess acetonitrile) before being dissolved in water and placed in a dialysis membrane. The product was dialyzed against water for 5 days before being freeze-dried and stored at 4 °C for further use.

2.5. Preparation of pre-crosslinked hydrogels (single crosslinker system)

In a 4 mL vial, 300 mg of PE-Glyc80 were added, followed by gradual additions of 10-fold (10X) Phosphate Buffered Saline (PBS), ultra-pure water and ammonium hydroxide (NH_4OH, 1 M) as an acidity balancing agent. The result was a 30% w/v polymer solution. 57.7 µL of PEGDMA750 were added to the solution, followed by 30 mg of GelMA (DoF 45%). Finally, Eosin Y (8.88 µL from a 2 mg/mL aqueous stock solution) and triethanolamine (5.12 µL from a 500 mg/mL aqueous stock solution) as the initiation system were added. The mixture was degassed with N_2 for 3 min and exposed to visible light from a multi-wavelength, 300 W lamp until a soft gelatinous consistency was achieved (so that the gel would be able to be aspirated into a syringe and later extruded during 3D printing). For the laponite-containing gels, 2.5 mg of laponite (0.5% w/v) were introduced to the reaction mixture prior to the addition of triethanolamine and Eosin Y. The mixture was stirred until adequate dispersion of the

nanoclay was achieved. Afterwards, the initiating system (triethanolamine, Eosin Y) were added in the aforementioned quantities, and the same procedure was followed.

2.6. Preparation of pre-crosslinked hydrogels (double crosslinker system)

In a 4 mL vial, 300 mg of PE-Glyc80 were added, followed by gradual additions of 10-fold (10X) Phosphate Buffered Saline (PBS), ultra-pure water and ammonium hydroxide (NH_4OH, 1 M) as an acidity balancing agent. The result was a 30% w/v polymer solution. 57.7 µL of PEGDMA750 were added to the solution, followed by 30 mg of GelMA (DoF 45%). Finally, Eosin Y (8.88 µL from a 2 mg/mL aqueous stock solution) and triethanolamine (5.12 µL from a 500 mg/mL aqueous stock solution) as the crosslinking initiation agents. The mixture was degassed with N_2 for 3 min and exposed to visible light from a multi-wavelength, 300 W lamp until a soft gelatinous consistency was achieved (so that the gel would be able to be aspirated into a syringe and later extruded during 3D printing). For the laponite-containing gels, 2.5 mg of laponite (0.5% w/v) were introduced to the reaction mixture prior to the addition of triethanolamine and Eosin Y. The mixture was stirred until adequate dispersion of the nanoclay was achieved. Afterwards, the initiating system (triethanolamine, Eosin Y) were added in the aforementioned quantities, and the same procedure was followed.

2.7. Cell culture of Pre-osteoblasts (carried out by Konstantinos Loukelis)

MC3T3-E1 pre-osteoblastic cells (DSMZ, Braunschweig, Germany, ACC-210) isolated from newborn mouse calvaria have the capacity to differentiate into osteoblasts in vitro, and have been used for the investigation of cell adhesion, viability, proliferation, and differentiation of biomaterials. The pre-osteoblastic cells were cultured in complete medium comprising alpha-MEM cell culture medium supplemented with 10% (*v/v*) fetal bovine serum (FBS), 100 µg/mL penicillin and streptomycin, 2 mM L-glutamine, and 2.5 µg/mL amphotericin in a humidified incubator at 37 °C, 5% CO_2 (Heal Force, Shanghai, China). The culture medium was replaced twice weekly. The cells were detached using trypsin-0.25% ethylenediaminetetraacetic acid (EDTA). Passages 12–17 of pre-osteoblastic cells were used for the viability experiments.

2.8. 3D Printing of the pre-crosslinked hydrogels

For the incorporation of cells within the crosslinked gels (i.e. the transition from plain “ink” to “bio-ink”), 1 mL of pre-crosslinked gel was aspirated into a syringe. For this amount of material, a 100 µL MC3T3-E1 pre-osteoblastic cell suspension was aspirated into a second syringe. The two syringes were joined through a female/female Luer lock, and the two components were mixed through pressing the plungers back and forth. The same procedure was followed for polyester- as well as polyester/laponite-based hydrogels. Once adequate mixing was accomplished, the resulting gels were loaded into a 5 mL printer cartridge equipped with a pneumatic plunger through a female/female Luer lock. The cartridges were then loaded onto the 3D printer (Inkredible, Cellink, Figure 11) and extruded into the chosen structures.

Figure 11. The Inkredible+ series of bioprinters by Cellink

2.9. Cell viability assessment within the hydrogels (carried out by Konstantinos Loukelis)

The cell viability cultured in the scaffolds was assessed using a live/dead assay following the manufacturer instructions. Briefly, the pre-osteoblastic cells were seeded in direct contact with the materials, and after 1 and 7 days of culture they were washed with PBS and then incubated in a working solution containing 2 mM calcein-AM (494 nm excitation/517 nm emission) and 4 mM ethidium homodimer III (EthDIII) (532 nm excitation/625 nm emission)

at room temperature for 45 min. The stained cells were observed under an inverted fluorescence microscope. Visualization of the fluorescently labelled cells was performed using the ImageJ software (ImageJ software, sLOCI, University of Wisconsin, Madison, WI, USA).

2.10. pH-dependent hydrogel swelling studies

To investigate the effect of the solution pH on the degree of swelling of the produced hydrogels, 50-100 mg of the extruded hydrogels were soaked in PBS overnight to remove any unreacted components. Following soaking, the hydrogels were rinsed for 1 hr in UltraPure water. After rinsing, excess water was removed and the hydrogel pieces were dried overnight in a vacuum oven. Once dried, the hydrogels were immersed in vials containing in 3-4 ml of solutions set at pre-determined pH values (3.0, 6.0 and 9.0, and PBS at pH 7.4). For the execution of the swelling study, the hydrogels were removed from the corresponding buffers at certain time intervals, placed on absorbent paper to gently remove the excess buffer, and the mass of each swollen hydrogel was measured and noted. The swelling ratio at each time increment was calculated using the following formula (Park et al., 2009):

$$SR = \frac{W_s - W_d}{W_d}$$

Where, W_s is the mass of the swollen hydrogel and W_d is its corresponding dry mass. The result was then multiplied by 100 to acquire the degree of swelling (%). The experiment was performed for the single, as well as the double crosslinker hydrogels. Swelling studies for both types of hydrogels were performed in duplicates.

2.11. Hydrogel degradation studies

To investigate the degradation profile of the two types of hydrogels, pieces of the produced hydrogels were soaked overnight in PBS to remove any unreacted components and rinsed in UltraPure water for 1 h. Next, the dried hydrogels were placed in sealed glass vials and

immersed in 10 ml PBS buffer at pH 7.4, overnight. The swollen hydrogels were weighed and their mass was recorded. After weighing, the temperature of the test vials was set at 37 ^{o}C using a thermostated water bath. Then, at certain time intervals, namely 1, 7, 14 and 21 days, the hydrogels were removed from the buffer, gently dried on absorbent paper to remove the excess PBS, and the mass of the swollen hydrogel was measured and noted. The degree of degradation (% weight loss, WL) of each hydrogel was calculated as following (Mallandrich et al., 2017):

$$WL\,(\%) = \frac{W_i - W_d}{W_i}\,100\%$$

Where, W_i is the initial mass of the swollen hydrogel and W_d is the mass measured at different time intervals. Degradation studies for both hydrogel types were performed in duplicates.

2.12. Characterisation Techniques

2.12.1. Size Exclusion Chromatography (SEC)

In this particular technique, molecules are separated based on their size while passing through a column which consists of beads of different sizes pore. The sample is loaded into the column, along with a solvent (mobile phase). Molecules of smaller size can more easily permeate the pores, getting caught up inside them and making a delayed exit, while larger molecules do not fit inside the pores and pass by them, then being eluted in the void volume passing through the column. It is a useful method to determine the polymer molecular weight distribution except for the average molar mass.

The polyesters' molecular weights and distributions were assessed using Size Exclusion Chromatography (SEC) employing a Waters-515 isocratic pump with two columns, Mixed-D and Mixed E from Polymer Labs. Detection was conducted with a Waters 2745 Dual

Absorbance detector and a Waters 410 refractive index (RI) detector (Figure 12). The eluent used was Tetrahydrofuran (THF) with 2 v/v% triethylamine (TEA) at a flow rate of 1 ml/min. Since SEC is a relative technique, molecular weights were determined via the universal calibration method, utilizing eight narrow molecular weight PMMA standards ranging from 875 to 138,600 gr/mol.

Sample preparation for size exclusion chromatography involved dissolving 10 mg of the synthesized polymer in tetrahydrofuran (THF), filtering the solution through a PTFE syringe filter, and injecting the sample through the injection valve.

Figure 12. A Waters® Size Exclusion Chromatography (SEC) machinery set-up.

2.12.2. Proton Nuclear Magnetic Resonance (^{1}H NMR) Spectroscopy

Nuclear magnetic resonance spectroscopy is a non-destructive analytical technique that can give information about the chemical structure of organic compounds. Certain nuclei, namely nuclei possessing an odd number of protons (^{1}H, ^{19}F, ^{31}P) or neutrons (^{13}C) and hence have half-integer spins, can possess specific magnetic properties and be considered as NMR-active nuclei. Thus, when a sample is placed in the strong magnetic field of an NMR spectrometer, half-integer spin nuclei are aligned. The sample is then subjected to radiofrequency that causes excitation of the nuclei from a lower energy level to a higher one. When the radiation

stops, the relaxation of the nuclei gives out a signal characteristic of each isotope that is converted to a spectrum. Different bonding patterns and different atoms that are close to the excited atomic nuclei can change the intensity of the radiation they experience, shifting the resonant frequency (chemical shift, translated as different positioning of the peaks on the x axis of the spectrum).

Sample preparation for proton Nuclear Magnetic Resonance spectroscopy involved dissolving about 15 mg of the synthesized polymer in deuterated chloroform (for p[TPAE-*alt*-AD]) or deuterated acetone (for PE-GlycX). The solution was transferred to a glass NMR tube, a magnetic spinner was affixed to the sample tube, and the sample was inserted into the instrument (Figure 13).

Figure 13. A Bruker® 500 MHz NMR spectrometer.

2.12.3. Scanning Electron Microscopy

Scanning Electron Microscopy (SEM) is an advanced imaging technique used to examine the surface morphology of samples at high magnifications. It works by scanning a focused electron beam over the sample's surface and detecting various signals, such as secondary electrons (SE) and backscattered electrons (BSE), to generate detailed images. SEM offers advantages such as high resolution, large depth of field, and the ability to analyse conductive

and non-conductive samples. However, it requires proper sample preparation, including coating with a thin layer of conductive material, and has limitations such as the potential sample damage from the electron beam radiation. Despite these challenges, SEM is widely used in various fields for its ability to provide valuable insights into the microstructure and properties of materials at the nanoscale.

The samples analysed in the Scanning Electron Microscope (Figure 14) were hydrogels created through two crosslinking approaches described below, and subjected to swelling studies in different pH conditions. Sample preparation for SEM involved immobilizing the freeze-dried samples upon a glass microscope slide with the aid of carbon tape, and rendering them conductive by coating them with gold through sputtering.

Figure 14. A JEOL JSM-IT710HR InTouchScope™ scanning electron microscope.

3. Results and Discussion

3.1. Synthesis of poly[TPAE-alt-AD]

The polymer synthesized in the experiments described here is an alternating co-polymer, a polyester product of a condensation reaction between trimethylolpropane (mono)allyl ether (TPAE) and adipoyl chloride (ADC) (Figure 15). The reaction is a solution polymerisation, where both the monomers and the end-product are soluble in a solvent, namely dichloromethane (DCM) in this case.

Adipoyl Chloride ($(CH_2CH_2C(O)Cl)_2$) is a compound with two acyl chloride molecules. It can react with water to form adipic acid.

Trimethylolpropane monoallyl ether ($H_2C=CHCH_2OCH_2C(C_2H_5)(CH_2OH)_2$) is a diol possessing two hydroxyl groups, through which it can engage in a polycondensation reaction, as well as an -ene group that, after condensation, ends up as a side group of the polymer's repeating unit.

During polycondensation, these two monomers form the repeating unit, resulting in the loss of a HCl molecule. Accumulation of this acid can cause the newly formed polyester chains to degrade. Thus, the weak base pyridine is used as an a HCl acceptor, forming a salt that can be easily removed via filtration (Yan and Siegwart, 2014). The end product is an aliphatic polyester with -ene side groups that, contrary to other polyesters, is amorphous, with an appearance and viscosity resembling that of room-temperature honey.

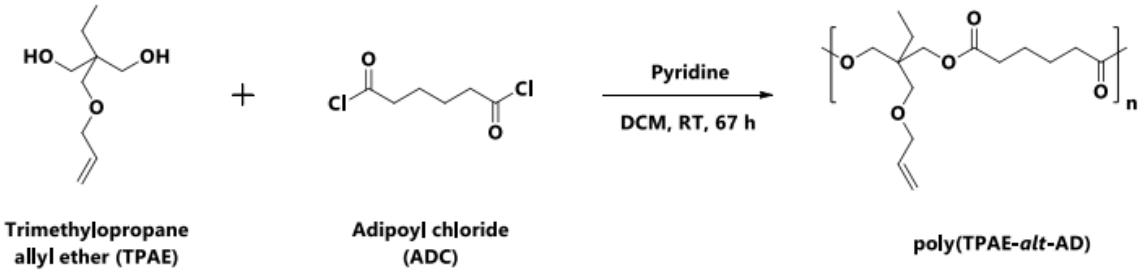

Figure 15. Overview of the p[TPAE-alt-AD] polycondensation reaction.

3.2. Structural and chemical characterisation of p[TPAE-alt-AD]

The polyester p[TPAE-alt-AD] was synthesized by a polycondensation reaction between TPAE, an alkene functionalised diol, and ADC, a diacyl chloride. The reaction time was approximately 67 h, after which the reaction flask was opened and the product was isolated by precipitation in cold methanol, and subsequently dried.

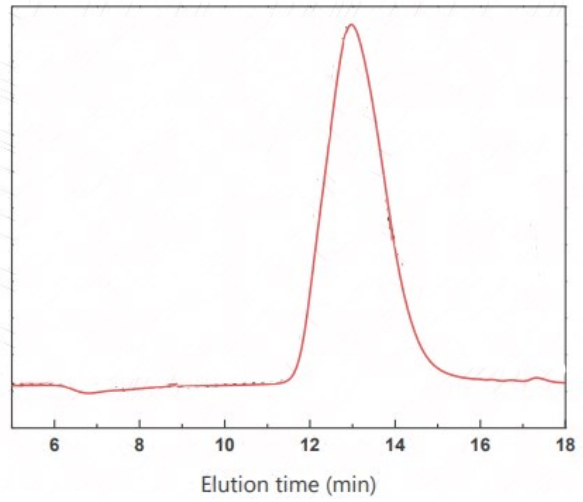

Figure 16. GPC/SEC of p[TPAE-alt-AD] with a molecular weight M_n = 36000 g/mol

SEC analysis of the synthesized polymer (Figure 16) revealed a number average molar mass M_n = 36,000 g mol^{-1} and a molecular weight distribution of M_w/M_n = 1.3. These measurements were taken post-precipitation in methanol, meaning that excess chloride and lower MW oligomers were dissolved in the supernatant and thus discarded.

^{1}H NMR spectroscopy (Figure 17) was also used to confirm the successful synthesis of p[TPAE-alt-AD]. Two characteristic peaks at 1.63 and 2.32 ppm can be seen in the spectrum of the polymer (protons labelled “e” and “d” in the spectrum below), attributed to the adipoyl monomer repeat unit. When it comes to the TPAE monomer repeat unit, there are two peaks at 5.82 and 5.0-5.2 ppm (protons labelled “h” and “i”) corresponding to the protons on each side of the double bond (vinyl group of TPAE).

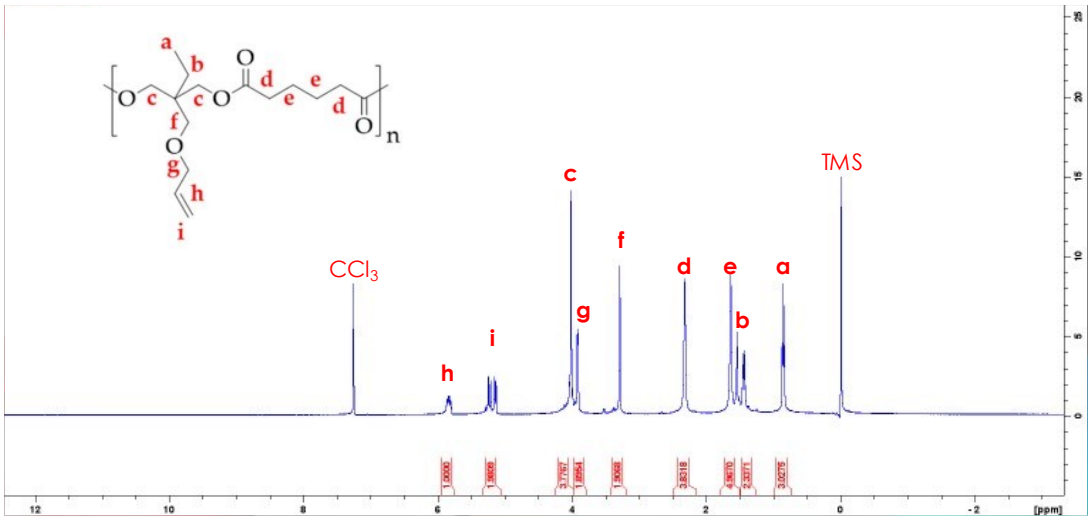

Figure 17. ^{1}H NMR spectrum of p[TPAE-alt-AD]. Peaks labelled “$CHCl_3$” and “TMS” are attributed to chloroform and tetramethylsilane, the sample solvent and internal calibration standard, respectively.

3.3. Structural characterisation of the carboxylic acid- functionalised polyesters

The previously synthesized polyester is hydrophobic and relatively inert, meaning that it would not be a suitable material to make scaffolds out of. That said, the -ene groups provide immense modification potential, meaning that various reactions can be utilised to add or substitute the allyl groups of the polyester's repeating unit. It is suggested by existing literature (Mountaki et al., 2021) that a facile and quick thiol-ene "click" reaction using mercaptocarboxylic acids can be exploited to endow the polymer with carboxylic acid side groups, making it more hydrophilic and giving it pH-responsive properties in the process.

The double bond-containing polyester was functionalised post-synthesis with carboxylic acid pendant groups through a UV light-induced thiol-ene "click" reaction (Figure 18). For this reaction, thioglycolic acid, containing two carbon atoms, was used to react with the polyester. The reaction was carried out at room temperature with the aid of a UV lamp set at a wavelength λ = 365 nm, with DMPA as the free radical photoinitiator.

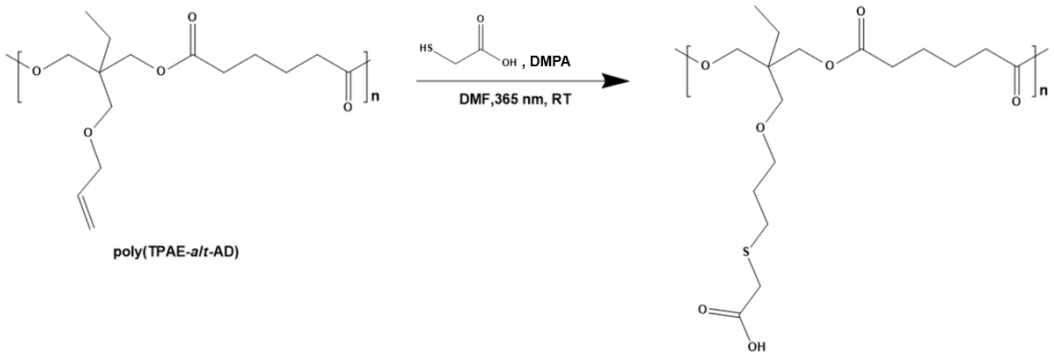

Figure 18. Overview of the thiol-ene "click" functionalisation reaction of p[TPAE-alt-AD]

To gain full temporal control of the reaction and the degree of functionalisation of the polymer, different means of introducing thioglycolic acid as well as degassing and irradiation times were studied (Table 1). It was deduced that the preferred method of introducing thioglycolic acid to the reaction mixture was with the aid of a micropipette, and that degassing all of the reagents together while being stirred was sufficient to ensure an oxygen-free N_2 atmosphere in the reaction flask. When using a syringe to introduce thioglycolic acid to the

reaction mixture the measuring accuracy was compromised, both by the syringe's graduation system and by the slightly corrosive properties of thioglycolic acid. This could explain the discrepancy between the results obtained when a 1 ml syringe was used.

At the same time, excessive degassing can significantly alter the volume of the reaction mixture, as evaporation can occur rapidly. Separate degassing, during which the volume of one component volume is even more compromised, decreased reproducibility between two reaction replicates which would otherwise appear identical, and was thus not used.

A 5x reaction scale (1.0 g of polymer) is a manageable and replicable amount of polymer, yielding satisfactory quantities of functionalised polymer that can later be used for further experimentation.

When it comes to irradiation time under the UV lamp, taking into consideration the ambient conditions (stirring, sunlight and room lights, distance between the lamp and the flask) and the irradiation source, an irradiation time of 140 seconds with the flask in direct contact with the lamp was found ideal to obtain a polymer with 80% functionalisation. The irradiation time intervals and the acquired degrees of functionalisation were not proportional, though it can be generalised that higher irradiation times yield higher degrees of functionalisation. That said, it is recommended that the irradiation time used for any desired degree of functionalisation should be first tested with smaller scale reactions, as different UV lamps and of different wattage and power can yield immensely different results. Experiments conducted in succession to those presented in the following table required increasingly longer amounts of time to successfully yield higher degrees of functionalisation, reflecting the wear of the irradiation source.

Polymers containing carboxylic acid side groups, such as the functionalised polyester mentioned here, are not soluble in THF. Since specific column and solvent combinations (that were not available in the lab) are required for the study of these compounds, ^{1}H NMR spectroscopy was chosen as the sole characterisation method to determine the success of the modification reaction

In comparison to the precursor p[TPAE-alt-AD] polymer, the spectrum of the functionalized polymer (Figures 19, 20 and 21) showed three new peaks at 1.85, 2.72 and 3.25 ppm (protons labelled "h'", "i'" and "j", respectively), corresponding to the newly formed thio-ether groups

of the polymer. The degree of functionalisation was calculated by ratioing the integral of the methylene protons of the polymer backbone (labelled “a”) at 0.89 ppm over the integrals of the peaks of the remaining vinyl (double bond) protons (labelled “h” and “i”).

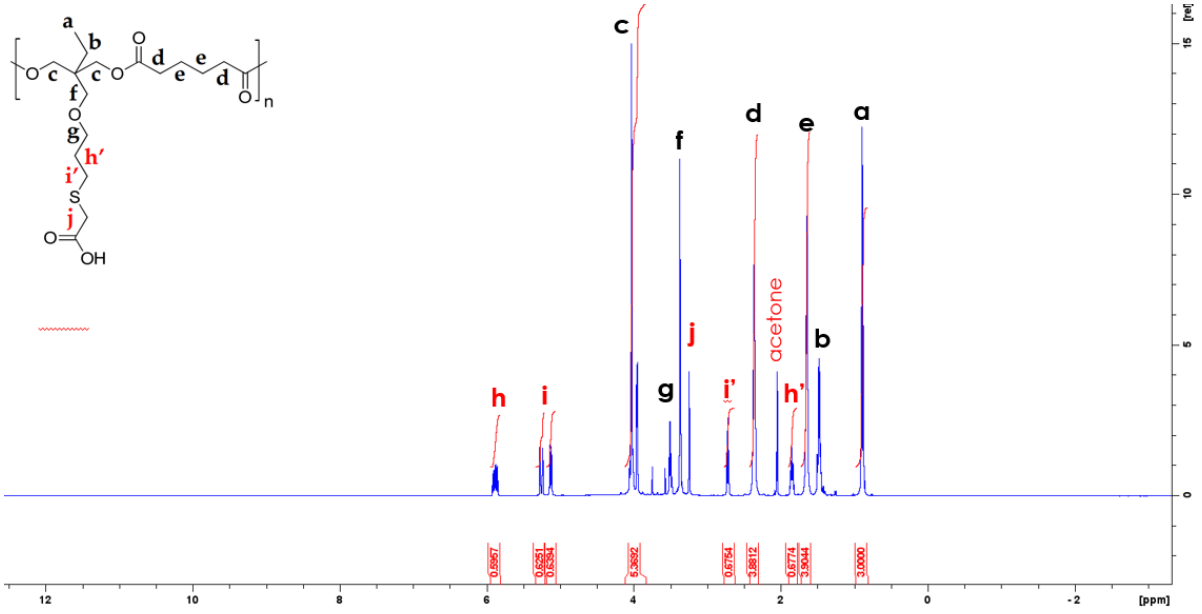

Figure 19. ^{1}H NMR spectrum of p[TPAE-alt-AD] functionalised by about 40%, obtained through MeOH dialysis

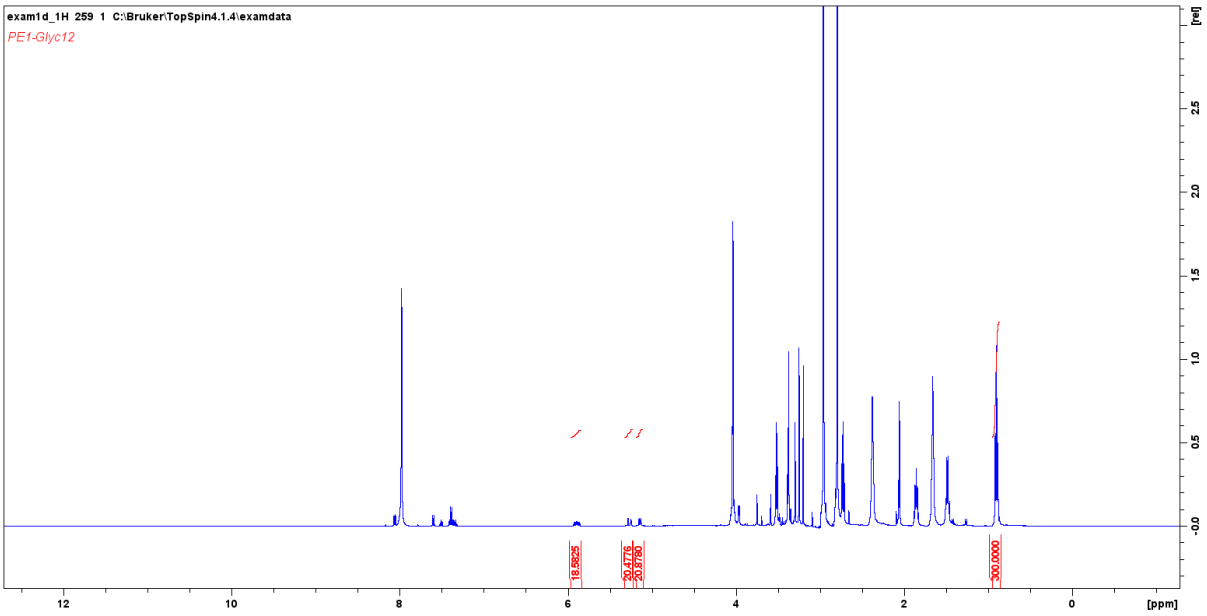

Figure 20. [1]H NMR spectrum of p[TPAE-alt-AD] functionalised by 80%, obtained by Hex/Eth precipitation. Note the extra peaks corresponding to DMPA (peaks around 7.50 ppm) and DMF (peaks at 8.00, 2.97 and 2.88 ppm) as a result of the rapid precipitation -and thus inadequate purification- of the product.

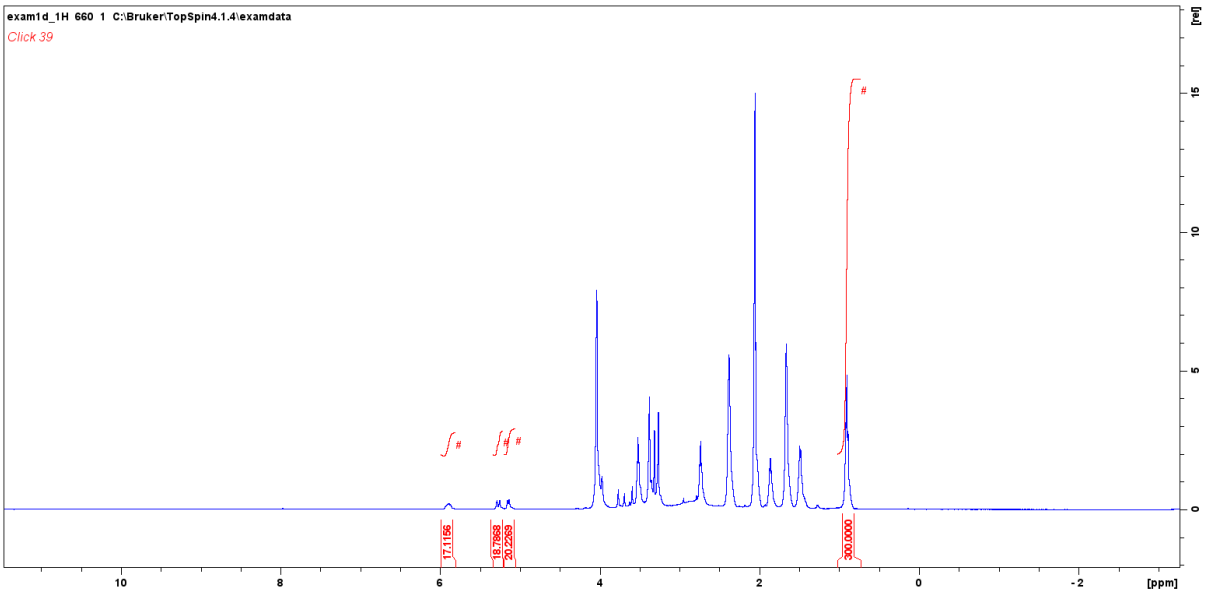

Figure 21. [1]H NMR spectrum of p[TPAE-alt-AD] functionalised by 80%, obtained by precipitation in methanol. Note the absence of solvent and initiator peaks mentioned in the previous figure, indicating a cleaner product.

Table 1. Overview of conditions tested for the functionalisation reaction of p[TPAE-alt-AD] with thioglycolic acid.

Reaction	*Irradiation time (s)*	*Method of thioglycolic acid addition*	*Method of product isolation*	*Functionalisation (%)*	*Comments*
PE-Glyc(1)	60	Micropipette	MeOH dialysis and Hex/Eth precipitation	40	Bulk degassing
PE-Glyc(2)	60	Micropipette	MeOH dialysis and Hex/Eth precipitation	45	Bulk degassing
PE-Glyc(3)	80	Micropipette	MeOH precipitation	40	Bulk degassing
PE-Glyc(4)	80	1 ml syringe	Hex/Eth precipitation	60	Separate degassing
PE-Glyc(5)	100	1 ml syringe	Hex/Eth precipitation	45	Separate degassing
PE-Glyc(6)	200	Micropipette	Hex/Eth precipitation	100	Separate degassing
PE-Glyc(7)	140	Micropipette	MeOH precipitation	75	Separate degassing
PE-Glyc(8)	140	Micropipette	Hex/Eth precipitation	94	Separate degassing
PE-Glyc(9)	100	Micropipette	Hex/Eth precipitation	75	Separate degassing
PE-Glyc(10)	100	Micropipette	Hex/Eth precipitation	70	Separate degassing
PE-Glyc(11)	110	Micropipette	Hex/Eth precipitation followed by MeOH precipitation	63	2.5x scale (0.5g of polyester)
PE-Glyc(12)	140	Micropipette	Hex/Eth precipitation followed by MeOH precipitation	80	5x scale (1g of polyester)
PE-Glyc(13)	140	Micropipette	Hex/Eth precipitation	80	5x scale (1g of polyester)

Note: "Separate degassing" refers to the reaction mixture containing p[TPAE-alt-AD], DMF and DMPA being degassed at the same time, with thioglycolic acid being degassed in a separate container and added to the reaction mixture post-degassing.

3.4. Synthesis of gelatin methacrylamide

The successful functionalisation of gelatin towards gelatin methacrylamide was verified by proton nuclear magnetic resonance (NMR) spectroscopy. Gelatin methacrylamide consists of gelatin modified to bear methacrylic moieties, whose presence is reflected in the appearance of new peaks in the respective NMR spectra (Pepelanova et al., 2018) (Figure22). The new peaks correspond to the methyl and methylene protons of the methacrylate unit. Methylene protons appear as two peaks at approximately 5.40 ppm and 5.65 ppm, while the methyl protons correspond to a sharp, prominent peak at approximately 1.90 ppm.

For gelatin, the methacrylation reaction generally occurs at available lysine (*Lys*) and aspartate (*Asp*) residues. Therefore, the degree of functionalisation of gelatin methacrylamide (GelMA) was calculated by comparing the integrals of the peaks corresponding to the lysine (3.00 ppm) and aspartate (2.72 ppm) residual protons, and comparing them to the integral of the peak corresponding to the phenylalanine protons (*Phe*, 7.30 ppm) (Zhu et al., 2019) which remain constant. The resulting fraction of *Lys* and *Asp* residues was then compared with that of the non-functionalised gelatin to determine how many residues had remained unreacted during by the methacrylation reaction, and allowed to determine the degree of functionalisation of the biopolymer (Table 2).

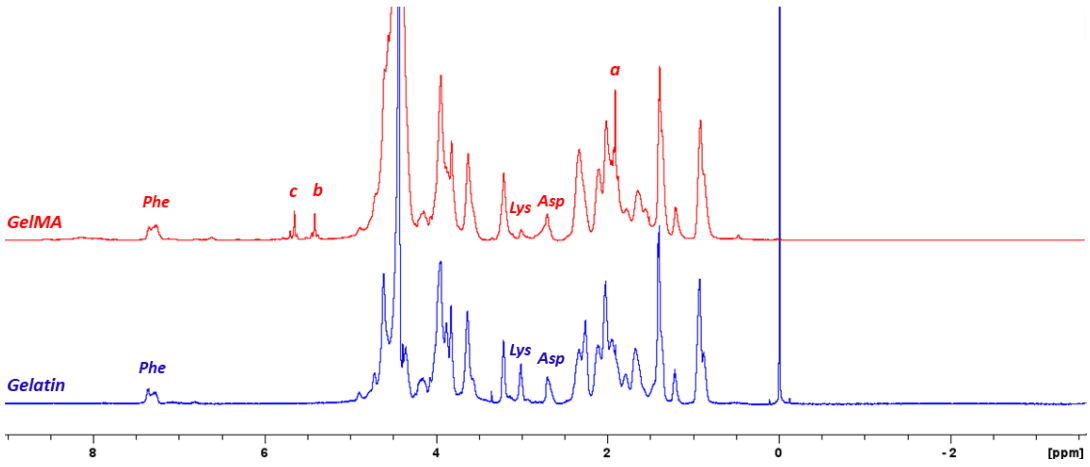

Figure 22. NMR spectra of unmodified gelatin (red) and GelMA (blue)

Table 2. Integral values of unmodified gelatin and gelatin methacrylamide (GelMA), obtained via ^{1}H NMR spectroscopy.

Sample	***Phenylalanine Integral***	***Aspartate Integral***	***Lysine Integral***	***Aspartate DoF***	***Lysine DoF***	***Average DoF***
Gelatin	5	3.93	3.52			
GelMA	5	2.51	1.87	36.1%	46.9%	41.5%

3.5. Synthesis and 3D Printing of PEGDMA750- and PEGDMA750-GelMA-crosslinked hydrogels

As previously noted, tissue engineering relies significantly on bioactive biomaterial scaffolds that mimic and substitute real tissues. In pursuit of this goal, a carboxylic acid-functionalized polyester, PE-Glyc80, which demonstrated high cell viability compared to other previously studied polyesters, was employed to create 3D-printed materials using an extrusion-based technique.

PE-Glyc80 is a low T_g polymer at temperatures around room temperature, and generally has poor printing properties. One of the first approaches was to solubilise it and mix it with an appropriate crosslinking agent, as well as an initiation system. For this purpose, poly(ethylene glycol) dimethacrylate with an average M_n of 750 (PEGDMA 750) was chosen as the crosslinker for the 3D printing of the polyester, due to the presence of the two methacrylate groups that can react with the polyester's available vinyl bonds (Figure 24). As a proof-of-concept PE-Glyc80, PEGDMA750 and 2,2-dimethoxy-2-phenylacetophenone (DMPA) were dissolved in acetone and then irradiated with UV light (λ = 365 nm) until a firm gel was acquired. During the first trials, the combination of PE-Glyc80 at a 1:1 mole ratio of the polymer alkene groups to PEGDMA750 was used. After partial crosslinking, the hydrogels were loaded onto a syringe equipped with a 23G blunt needle, and the extrusion of the material was manually tested (Figure 23). After extrusion, all resulting scaffolds were additionally cured under UV light to obtain a non-flowing hydrogel.

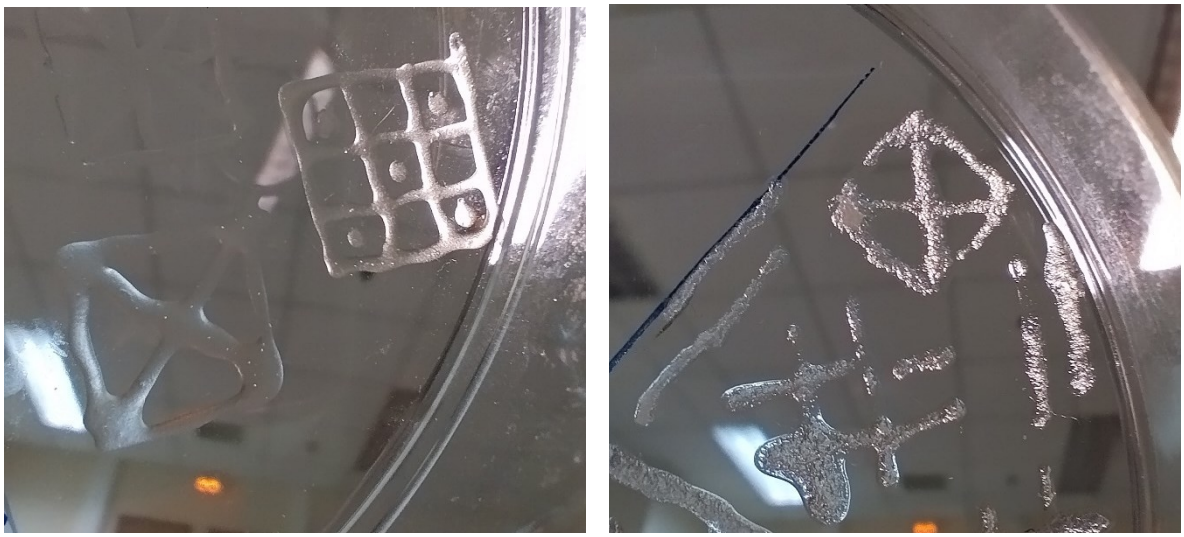

Figure 23 Hydrogels fabricated using PEGDMA750 as the crosslinker and DMPA as the UV-activated photoinitiator

Since the hydrogels were ultimately intented for use as Tissue Engineering scaffolds, the combination of acetone as solvent, along with a UV-activated photoinitiator and curing system, was deemed unsuitable for further experiments. Therefore, the solvent was changed to phosphate buffered saline (PBS), chosen for its isotonic, cell-friendly nature, as well as its wide use in cell and tissue culture experiments. However, the polyester was insoluble in this aqueous media. The presence of the carboxylic acid pendant groups rendered the functionalised polymer responsive to pH changes, being more hydrophilic at pH values above its pK_α at 6.5. For this, 10-fold concentrated PBS was used in tandem with a 1 M solution of ammonium hydroxide in Milli-Q water to achieve optimal dissolution and buffering properties of the polymer. Moreover, DMPA was replaced by a the visible photoinitiator system comprising Eosin Y as the photosensitiser dye and triethanolamine (TEOA). (Bahney et al., 2011, Wang et al., 2018, Sharifi et al., 2021)

The combination of Eosin Y and triethanolamine is a system that has been widely considered to be oxygen-tolerant. Since the hydrogel was intended for mixing with a cell suspension before extrusion, the concentration of the photoinitiator system was optimised to be high enough to be oxygen-tolerant, while at the same time low enough to ensure that viable cell growth could be attained. We found that an extremely low concentration of the initiating system was required (0.02 mM Eosin Y and 2% w/v TEOA) with additional degassing post-mixing, to ensure both successful gelation of the solution, as well as cell viability. After irradiation with white, multi-wavelength visible light, the resulting hydrogels were loaded

onto syringes equipped with a 23G blunt needle and manually extruded. Post-extrusion, all constructs were cured under visible light.

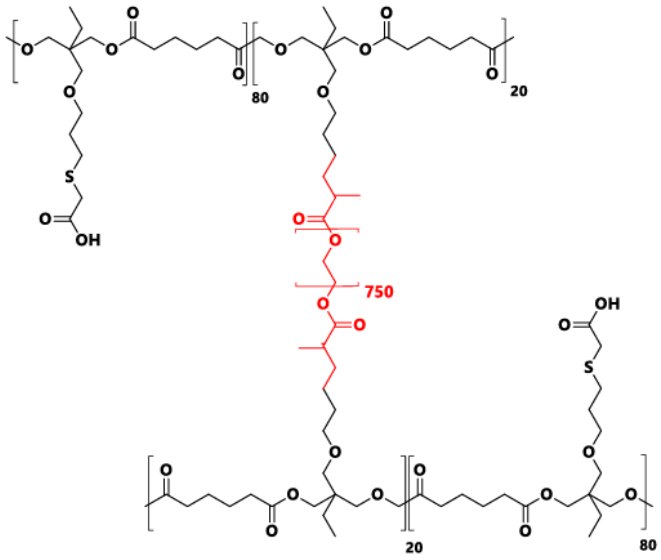

Figure 24. Schematic representation of a PEGDMA750-crosslinked polyester (PE-Glyc80) hydrogel

However, the use of PEGDMA750 as a sole crosslinking agent raised concerns regarding the cell-adhesive properties of the resulting hydrogels. Being a poly(ethylene glycol)-based polymer, PEGDMA750 is quite hydrophilic, and at the same time, it possesses anti-fouling properties (Liu et al., 2014). Thus, the search for a new crosslinking agent became necessary. GelMA was chosen due to its ease of production, cell-viability and richness in adhesive RGD peptide patterns (Kirsch et al., 2019).

GelMA was tested as a sole crosslinker (Figure 25), in a process identical to the one mentioned above. The functionalised biopolymer was dissolved in PBS containing ammonium hydroxide together with the polyester, Eosin Y and TEOA were added, the mixture was degassed and irradiated under visible light, and the resulting constructs were extruded through a 23G blunt syringe needle. Two types of GelMA were tested for this purpose (DoF 20% and DoF 42%). Due to its low methacrylic group content, 20% DoF GelMA produced loose viscous constructs that could not hold their shape in single layers, let alone in a multi-layered 3D-printed construct. One the other hand, 42% DoF GelMA produced relatively stiff hydrogels that could successfully hold their shape when extruded, but were still quite sticky and soft (Figure 25).

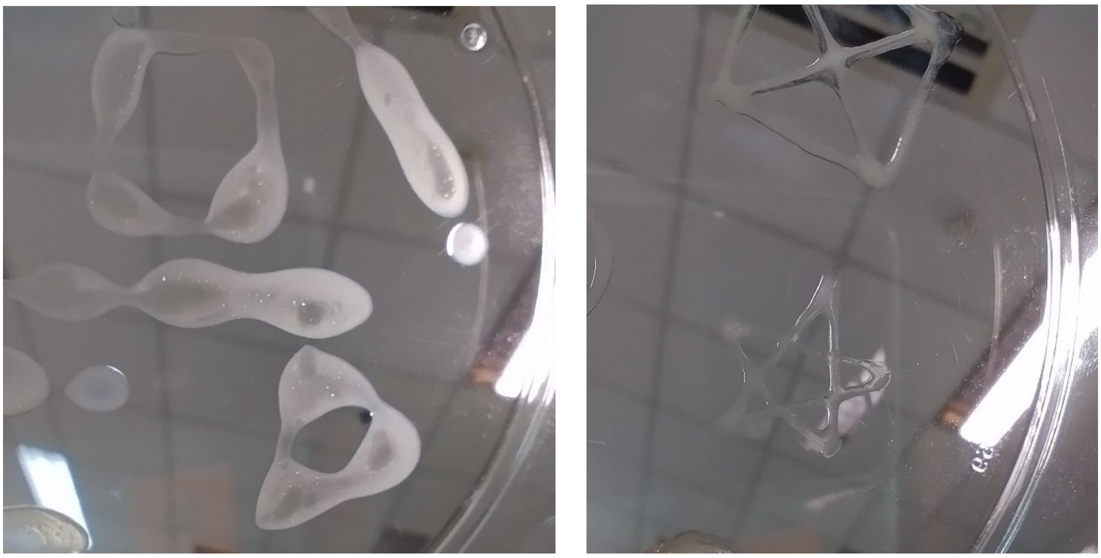

Figure 25. Polyester hydrogels obtained with GelMA (left: DoF 20%, right: DoF 42%) as the crosslinker

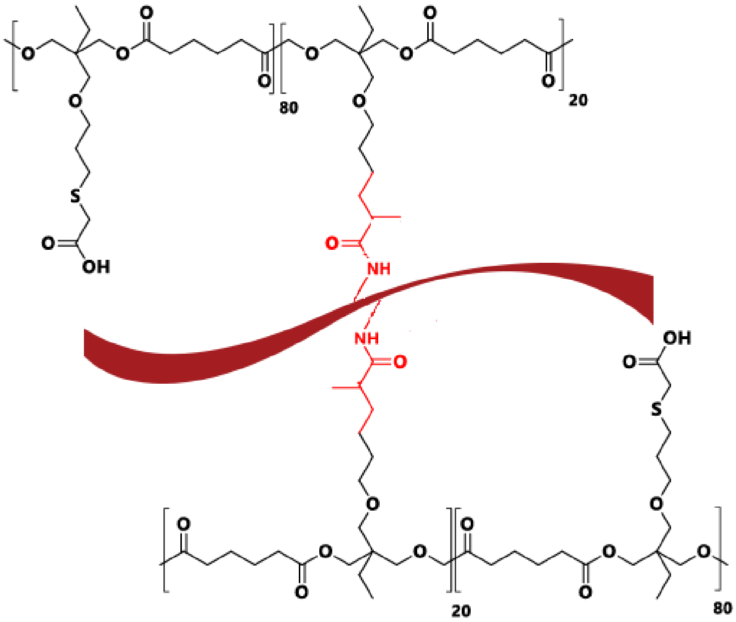

Figure 26. Schematic representation of a GelMA-crosslinked polyester (PE-Glyc80) hydrogel

Since a sole crosslinker did not manage to provide a hydrogel of adequate firmness and extrusion properties, PEGDMA750, used to exploit the excellent mechanical properties it provided to the hydrogel during extrusion, together with GelMA with DoF 42% were combined to obtain the polyester hydrogels. The concentration of PEGDMA750 was halved compared to its original value (~30% of the total polymer weight in solution), and was

supplemented by an equal amount of GelMA with DoF 42%. The solution was prepared as previously described, degassed and irradiated with visible light. The resulting hydrogels, however, displayed much of the GelMA cross-linked material properties, namely stickiness and low construct viscosity. Thus, the ratio of PEGDMA750 to GelMA was adjusted to 20% and 10% w/w, respectively to increase the firmness of the scaffolds. These hydrogels were found to retain the formidable mechanical properties displayed by the PEGDMA750-crosslinked hydrogels, while also containing a significant amount of GelMA which rendered the hydrogel suitable for cell adherence and growth (Figure 26).

Figure 26. A PEGDMA750-GelMA-crosslinked hydrogel (20%-10% w/w, respectively)

After establishing the printing parameters for the polyester (PE-Glyc80) hydrogels, the nanoclay laponite was added in the mixture under identical conditions as those described above to create hybrid polyester-laponite (PE/LAP) structures (Figures 27 and 28). Laponite was chosen due to its favorable properties, as it has been demonstrated that it enhances the printing precision, while at the same time serving as a crosslinker and boosting the scaffold's bioactivity in osteogenesis by promoting cell spreading and differentiation in the tissue engineering constructs.

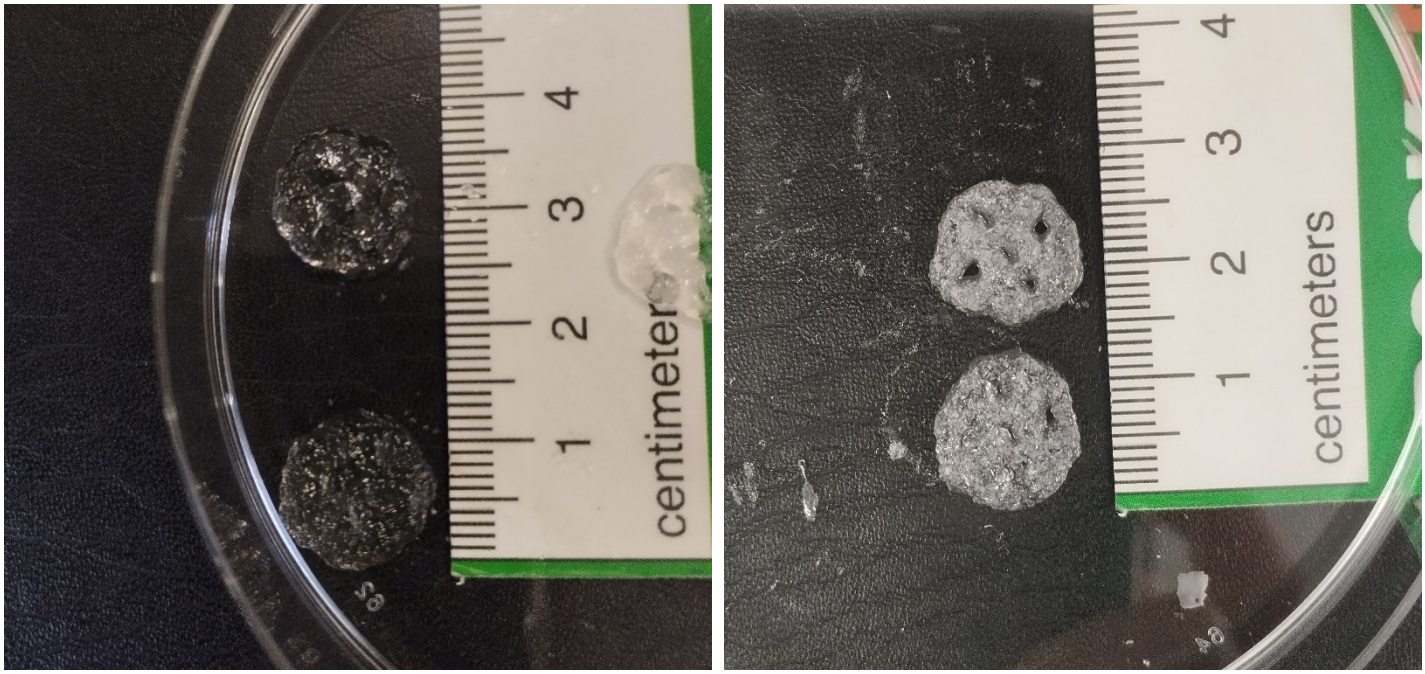

Figure 27. 3D-printed (PEGDMA 750-GelMA-crosslinked hydrogels with (right) and without (left) the addition of the nanoclay Laponite (0.5% w/v)

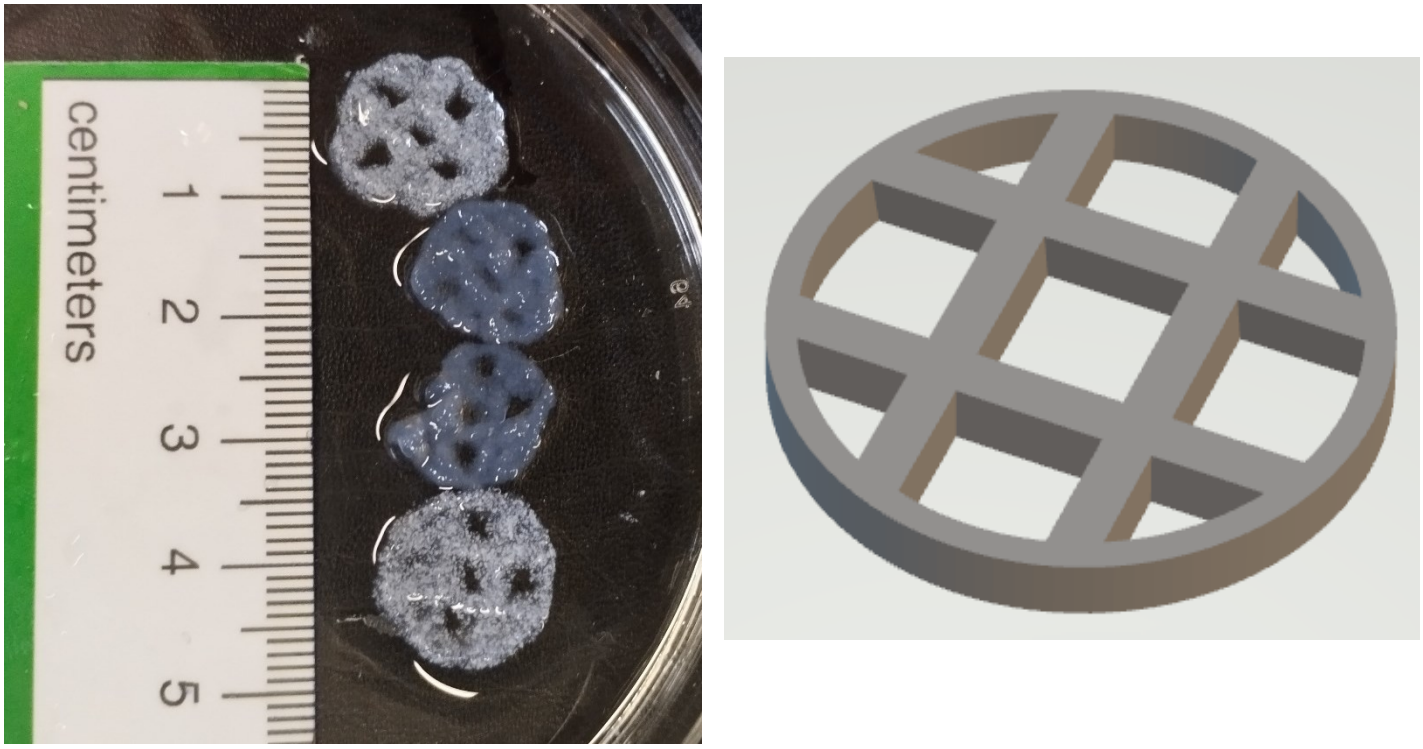

Figure 28. Laponite-containing (top and bottom) and non-containing (middle), PEGDMA 750/GelMA-crosslinked hydrogels after immersion in PBS, compared with the original digital design (right image)

3.6. pH-dependent swelling properties of the PEGDMA750- and PEGDMA750/GelMA-crosslinked hydrogels

Next, the swelling properties of the polyester hydrogels were examined as a function of the pH of the medium. For this, the hydrogels were immersed in solutions of different pH values and their degree of swelling was determined by gravimetric analysis. The solution pH was selected based on previously conducted potentiometric titrations by our group (Mountaki et al., 2021). In relatively strong acidic solutions (pH value of 3), the 80% functionalised polyester was fully protonated and insoluble in aqueous media. The effective pK_α value of the polyester was found around 6, hence a pH value of 6.5 was chosen for the swelling experiments. On the other hand, the polymer is soluble at alkaline media. Therefore, a pH value of 7.4 (PBS solution) was chosen to emulate the body's physiological conditions and a relatively strong alkaline solution (pH value of 10) was also investigated.

The following graphs show the swelling behavior of the hydrogels at the different pH values as a function of immersion time in the aqueous media. Since the pendant groups of the main polyester molecule contain carboxyl groups, at high pH values they are expected to deprotonate from -COOH to -COO^-. The presence of these anions in the hydrogel can lead to charge repulsion and thus increased swelling and pore size. Conversely, at low pH values, this deprotonation reaction is minimal to non-existent, leading to no charge repulsion and, thus, minimal swelling.

In general, both the PEGDMA750- and PEGDMA750-GelMA-crosslinked hydrogels displayed similar swelling properties (Figures 29 and 30). Significant swelling was observed at pH 6.5 and 10, due to the ionization of the pendant carboxylic acid groups of the polyester. The slight decrease in the degree of swelling found at pH 10 compared to pH 6.5 was attributed to the higher ionic strength of the solution at the higher pH value. On the other hand, the degree of swelling decreased at pH 3 when the methacrylic acid groups of the polymer become protonated and uncharged. It is noted that the hydrogels exhibited their lower degree of swelling in PBS at pH 7.4, which is attributed to the high ionic strength of the buffer solution (isotonic) contributing to the lower osmotic penetration of water within the hydrogel.

The above results are in good agreement with the visual inspection of the hydrogels as well as the scanning electron microscopy (SEM) images presented below (Figure 31).

At pH 3, pores of small diameter and shallow depth are visible throughout the surface of the freeze-dried hydrogels, with the PEGDMA 750/GelMA-crosslinked hydrogels displaying a slight increase in pore depth and diameter. These results are consistent with the calculated swelling degrees of the hydrogels, depicted in Figure for the PEGDMA 750-crosslinked hydrogels and Figure for the PEGDMA 750-GelMA-crosslinked hydrogels.

At pH 6.5, the pores of both types of hydrogels appear wider in diameter, as well as considerably deeper than at pH 3. For the PEGDMA 750-crosslinked hydrogels, the observed pores appear more abundant, albeit shallower than the pores observed on the PEGDMA 750-GelMA-crosslinked hydrogels.

At pH 7.4, in accordance with the respective degrees of swelling of both examined hydrogel types, where buffer absorption was relatively minimal, both hydrogels display numerous small and shallow pores, almost identical to the ones observed at a pH value of 3.

Finally, at pH 10, both hydrogel types exhibited an extensive pore structure, with pores larger than at any of the lower corresponding pH values. It is also notable that the pores observed on the surface of the PEGDMA 750-GelMA-crosslinked hydrogels appear much wider in diameter, as well as significantly deeper, which is also reflected in the considerable difference in maximal swelling degrees between the two hydrogel types.

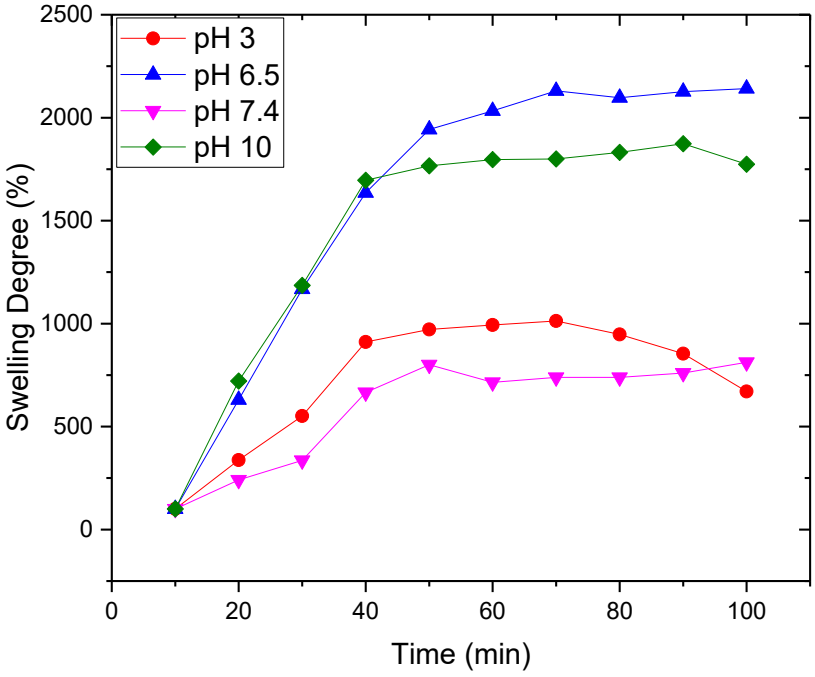

Figure 29. Degrees of swelling of the PEGDMA750-GelMA-crosslinked hydrogels as a function of immersion time in the aqueous media

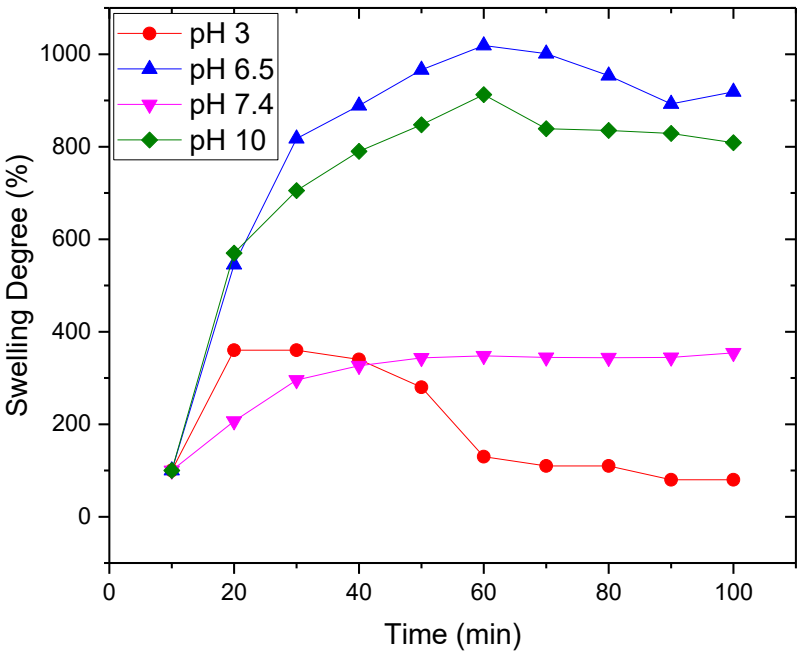

Figure 30. Degrees of swelling of the PEGDMA750-crosslinked hydrogels as a function of immersion time in the aqueous media

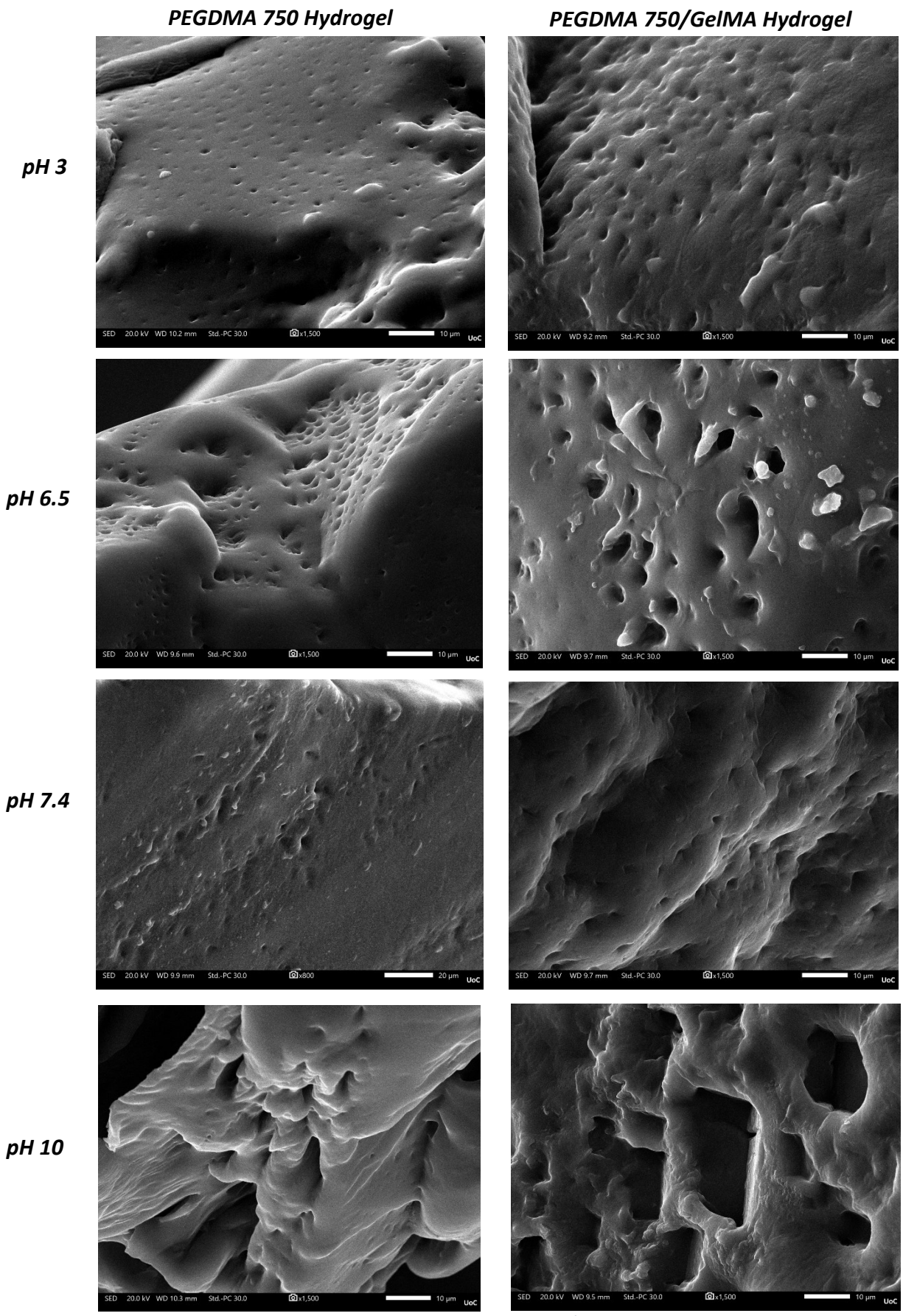

Figure 31. SEM images of PEGDMA 750- (left) and PEGDMA 750/GelMA- (right) crosslinked hydrogels after swelling studies in different pH values.

3.7. Degradation profiles of the PEGDMA750- and PEGDMA750/GelMA-crosslinked hydrogels

The degradation rates of the hydrogels play a pivotal role for their applications in tissue engineering, by providing the required mechanical support to the cells and influencing the cell behavior, biocompatibility and tissue integration ultimately contributing to the successful regeneration of a functional tissue. The ideal degradation time of hydrogels used in bone tissue engineering, depending on the application, should amount to at least 3 weeks, leaving an ample amount of time required for a traumatic injury, such as a bone fracture, to heal. Of course, the degradation kinetics of any given hydrogel, once implanted, are also greatly affected by the overall health and inflammatory status of the surrounding tissue. (Reid et al., 2015)

Hydrogels that degrade too slowly may impede the integration of new tissue into the surrounding native tissue. Relatively rapid degradation allows for the gradual replacement of the scaffold with newly formed tissue, promoting seamless integration. Degradation of the hydrogel scaffold also creates space for cell migration and proliferation within the tissue-engineered construct. Of equal importance is the fact that the degradation products of the hydrogel should be non-toxic and biocompatible to avoid adverse reactions or inflammation in the surrounding tissue. Controlled degradation ensures that the degradation products are safely metabolized or excreted by the body. Sometimes hydrogels can even be designed to degrade in such a way, that a bioactive product is created upon breaking down the hydrogel (Sindhu et al., 2020). Finally, while the hydrogel scaffolds provide initial mechanical support for cell attachment and tissue formation, they should gradually degrade to allow the newly regenerated tissue to bear mechanical loads and function properly. Balancing degradation with mechanical integrity is crucial for the successful tissue regeneration.

In this study, the degradation profile of both PEDDMA 750- and PEGDMA 750-GelMA-crosslinked hydrogels was investigated (Figure 32). After recording their initial mass while swollen, the hydrogels were immersed in PBS, pH 7.4 at 37^{o}C, and measurements were carried out at time intervals of 1, 7, 14 and 21 days (Figure). Both hydrogel types proved to be quite robust, as at the 21-day time increment, they had yet to exhibit any mass loss. On the contrary, both hydrogel types exhibited a slightly increased degree of swelling during testing, which was not comparable to the degrees calculated during the swelling study, but

noticeable nonetheless. This robustness and resistance to degradation during the first three weeks of the study could suggest materials that could be suitable for bone tissue engineering, though it is recommended that the degradation study go on in order to gain a more faithful and complete overview of the hydrogels' degradation kinetics.

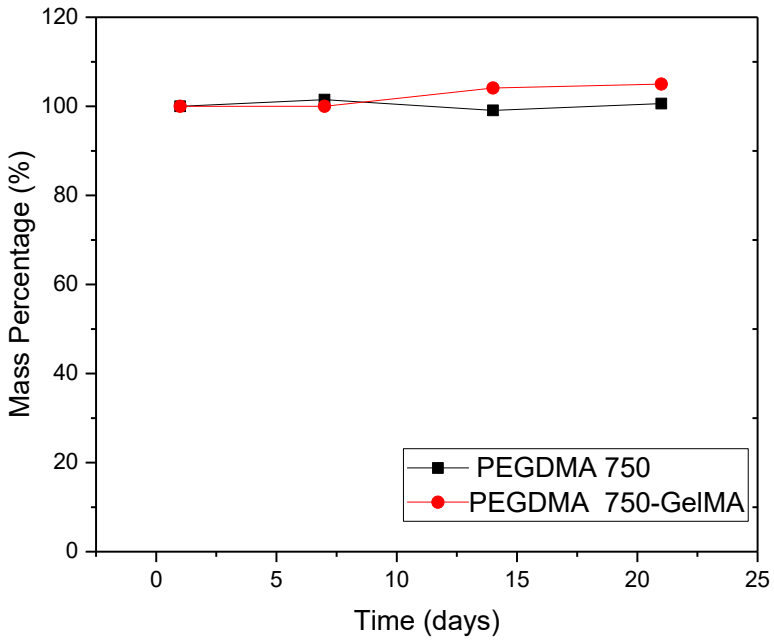

Figure 32. Degradation profile of PEGDMA 750- and PEGDMA 750-GelMA-crosslinked hydrogels at certain time intervals after immersion in PBS at 37ºC.

3.8. Evaluation of the Cell Viability in the Bioink

The cell viability was assessed by means of live-dead staining and imaging. Cells cultured within the PEGDMA 750-GelMA-crosslinked hydrogels (with and without the addition of laponite) for 1 and 7 days were stained with the live-dead assay and visualized under a fluorescence microscope (Figure 33). The resulting images from day 1 showed an especially increased number of seemingly dead cells, visualised in red from the ethidium homodimer.

This observation began to raise questions about the viability of cells in the presence of the ethidium homodimer, as it is in itself toxic and difficult to wash away once introduced into a cell sample, and may thus produce artifacts in the observable fluorescence. For this purpose, the decision was made to forgo the ethidium homodimer staining. Thus, for the generation of the fluorescence images from day 7, only calcein staining was performed, in order to eliminate the possibility of interference from the ethidium homodimer. However, in the resulting images from day 7, no live cells (normally visualised in green) could be detected.

This lack of cell viability could be attributed to a number of factors. Firstly, it is possible that the cells failed to remain alive during the mixing of the hydrogels with the cell suspension, effectively asphyxiating due to the density and firmness of the resulting bioink leading to little to no cell culture medium penetration within the hydrogel and thus, limited accessibility to oxygen and nutrients. Secondly, as the extruded constructs were subjected to curing with a multi-wavelength, visible light lamp (also emitting in the near-IR and UV spectra), cell death through heat and UV irradiation is also plausible. Therefore, the effect of a lower irradiation time should be examined. Lastly, a possibility exists that the concentration of the initiating agents is detrimental to cell survival. The current concentration was chosen based on an extensive literature search, during which two different initiator contents were widely cited; 0.01mM Eosin Y with 0.1% w/v TEOA (Bahney et al., 2011), and 0.02mM Eosin Y with 0.2% w/v TEOA (Wang et al., 2018). Of these two, the higher proposed concentrations of 0.02mM Eosin Y and 0.2% w/v TEOA was chosen, as a means to facilitate rapid polymer crosslinking. However, it has been demonstrated that relatively high concentrations of Eosin Y and TEOA can be toxic to cells, especially in the context of creating a bioink, where cells are expected to grow *inside* the scaffold, and are not just laid on its surface, where the photoinitiator concentration would not have such an immediate effect on cell viability. Therefore, testing of

the lowest possible photoinitiator concentrations, as reported by Bahney et al., is strongly recommended.

To combat the problem of cell asphyxiation, it is suggested that the hydrogels be diluted with a larger volume of cell suspension for the creation of the bioink. It would also be useful for the pre-crosslinking conditions to be examined. During pre-crosslinking, a looser, easier to manage pre-ink could be created that would still be able to retain its shape in a cell culture environment, while at the same time facilitating cell access to nutrients. Additionally, it is suggested that rheological studies be conducted on this bioink. The results from these studies could be compared to other existing bioinks from the literature that have been successful in enhancing cell development, and the properties of the bioink developed in this project could thus be adjusted to increase its prospects in supporting cell viability and proliferation.

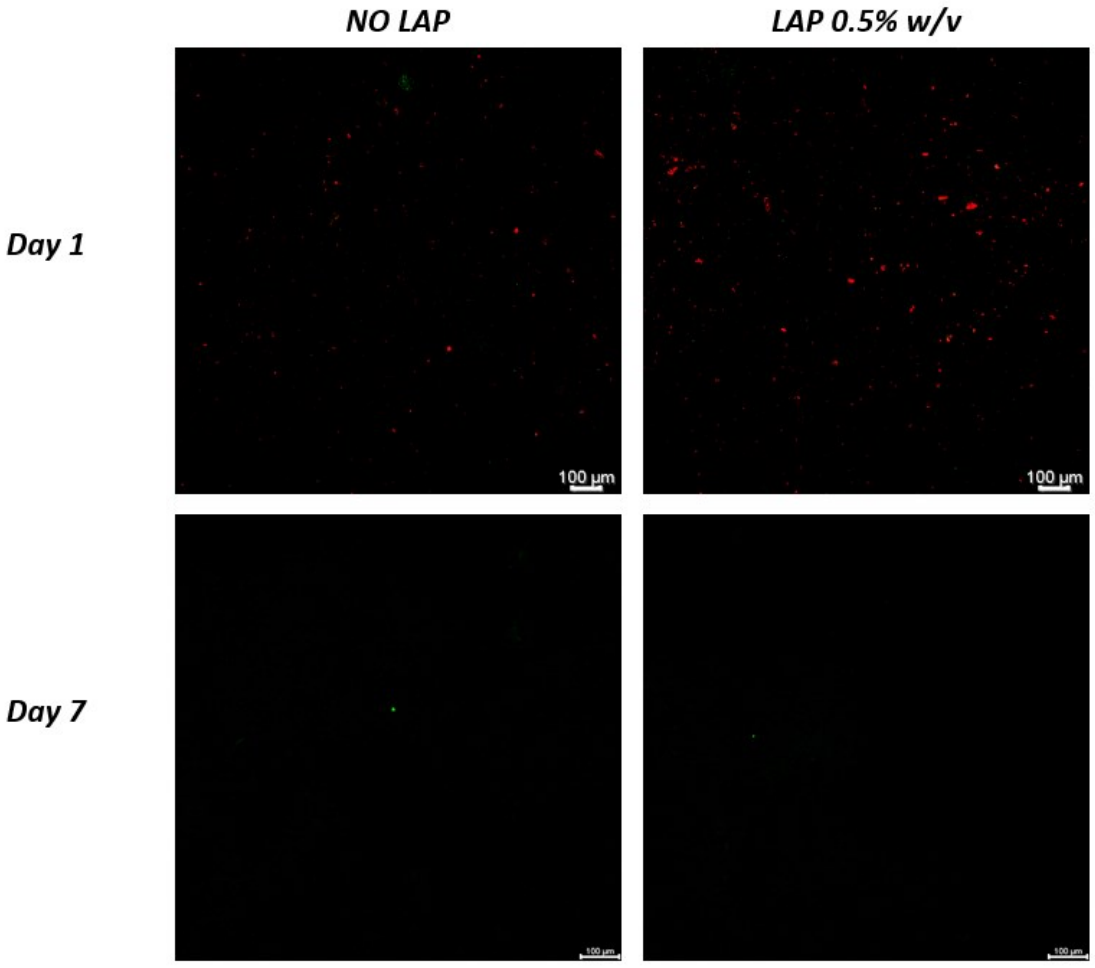

Figure 33. 1-day and 7-day live/dead cell viability assay, using calcein and ethidium homodimer to stain live (green) and dead (red) cells, respectively.

4. Conclusions

In this project, the creation of different hydrogel types is described, following the previously reported synthetic process of an aliphatic polyester with -ene side groups, formed through a condensation polymerisation reaction. The polyester's alkene groups were further modified through a UV-induced thiol-ene click reaction to endow the polymer with carboxylic acid pendant groups. For this purpose, thioglycolic acid was used to functionalise the initial polymer with acid side groups. A functionalization percentage of 80% was attained through careful fine-tuning of the time of the reaction mixture's exposure to UV light.

The inertness and hydrophobicity of the ene-bearing polyester do not render it attractive for use as a biocompatible scaffold for cell growth. However, the double bond side groups allow to easily functionalise the polymer via a quick, UV-mediated thiol – ene click reaction. The addition of thioglycolic acid replaced a large fraction of the -ene groups with carboxylic acid side groups, rendering the product more hydrophilic and granting it with pH-responsive properties. They also offer the possibility of covalently binding other compounds to the polymer, apart from thioglycolic acid, to combine responsive with bioactive properties on the polymer. These could be growth factors, small peptides or bioactive molecules such as drugs, as long as they possess a thiol or an amine group, that would aid in the ligation reaction.

In all cases, it is important to ensure that a fraction of double bonds remain available for chemical crosslinking of the polymer to create the desired bioink. Once gelation of the functionalised polyester has been attained, it is also possible to adsorb bioactive molecules onto it, either by mixing or incubating the hydrogel with a solution of the molecule in question. This could aid the functionalisation process by bypassing potentially complex chemical reaction steps, as well as avoiding the compromise of bioactive molecules by using potentially function-critical chemical moieties to covalently ligate them onto the polyester main chain, effectively decreasing, or even eliminating molecular activity.

Testing of different conditions, reaction scales and irradiation times resulted in the reproducible functionalisation of the polyester to bear 80% carboxylic acid moieties, suitable for cell growth, as suggested by our previous studies. At the same time, an approximate 20% of the product's double bonds are left intact, allowing the crosslinking of the polymer. The crosslinkers chosen for this project were poly(ethylene glycol) dimethacrylate with M_n = 750

g mol^{-1} (PEGDMA 750), both as a standalone crosslinking agent, as well as in combination with gelatin methacrylamide (GelMA) with a degree of functionalisation of 42%. The photosensitizer dye eosin Y and triethanolamine were chosen as a visible light, cell-friendly photoinitiation system based on a literature search. In summary, four types of hydrogels were prepared, based on their crosslinking agent, as well as the presence or absence of the nanoclay laponite. As the laponite content was quite low, and would thus not lead to noticeable differences in the swelling behavior and mass difference of the hydrogels, the swelling and degradation studies were conducted on laponite-free hydrogels with single and double crosslinking systems.

Regarding the cell viability studies, PEGDMA750 is generally regarded as an anti-fouling agent, and it was thus predicted that, despite the excellent extrusion properties and the ease of handling of its hydrogels, it would not be beneficial for cell growth when used as the sole crosslinker. Therefore, cell viability experiments were conducted with the PEGDMA750-GelMA double crosslinker hydrogels, using a cell suspension of MC3T3-E1 murine pre-osteoblasts. Viability was assessed via a live-dead calcein staining and observation using fluorescence microscopy. The results obtained raise questions about cell viability within the hydrogel, however this cannot be directly attributed to the unsuitability of the material itself, as some factors limiting cell growth, which are summarised below, could play a significant role. This paves the way for the future investigation of the prepared hydrogels.

The density of the hydrogel bioink could be higher than a certain threshold point yet to be determined, leading to cell asphyxiation due to the lack of space and culture medium penetration within the hydrogel. This could be combatted by further diluting the pre-crosslinked hydrogel with a larger volume of cell suspension. The bioink density problem could also be solved with the aid of rheological analyses, shedding light on the bioinks‘ mechanical properties and comparing it to ones that are already used successfully in research and industrial applications, so as to better tune the bioink’s dilution and subsequent properties. In addition to that, the irradiation dose applied on the diluted and casted hydrogels during curing may be detrimental to the cells, owing to the use of a multi-wavelength lamp that also emits infrared and ultraviolet light. Reduction of the curing time, or the use of wavelength cut-off filters could attenuate the effects of unwanted irradiation. Furthermore, it is also suggested that a lower quantity, namely half of the current

concentration of eosin Y and triethanolamine be used. In this project, the higher of two cell-suitable concentration combinations suggested in the literature was used. Future experiments on this bioink should make room for lower concentrations of the initiating factors to be utilised, at the expense of speed in obtaining the pre-crosslinked product. However, higher irradiation time during pre-crosslinking (i.e. before the cells are mixed into the hydrogel) is not expected to be harmful for cell growth and adhesion.

References

Acharya, R., Dutta, S. D., Patil, T. V., Ganguly, K., Randhawa, A., & Lim, K. T. (2023). A Review on Electroactive Polymer-Metal Composites: Development and Applications for Tissue Regeneration. Journal of functional biomaterials, 14(10), 523. https://doi.org/10.3390/jfb14100523

Armentano, I., Dottori, M., Fortunati, E., Mattioli, S., & Kenny, J. M. (2010). Biodegradable polymer matrix nanocomposites for tissue engineering: a review. Polymer degradation and stability, 95(11), 2126-2146.

Aqib Muzaffar, M. Basheer Ahamed, Kalim Deshmukh, Tomáš Kovářík, Tomáš Křenek, S. K. Khadheer Pasha, (2020) Chapter 4 - 3D and 4D printing of pH-responsive and functional polymers and their composites, 3D and 4D Printing of Polymer Nanocomposite Materials, Elsevier, Pages 85-117, ISBN 9780128168059

Aslam Khan MU, Abd Razak SI, Al Arjan WS, Nazir S, Sahaya Anand TJ, Mehboob H, Amin R. (2021) Recent Advances in Biopolymeric Composite Materials for Tissue Engineering and Regenerative Medicines: A Review. Molecules. Jan 25;26(3):619. doi: 10.3390/molecules26030619

Bahney, C.S., Lujan, T.J., Hsu, C., Bottlang, M., West, J.L., & Johnstone, B. (2011). Visible light photoinitiation of mesenchymal stem cell-laden bioresponsive hydrogels. European cells & materials, 22, 43-55; discussion 55 .

Bakhshandeh B, Zarrintaj P, Oftadeh MO, Keramati F, Fouladiha H, Sohrabi-Jahromi S, Ziraksaz Z. (2017) Tissue engineering; strategies, tissues, and biomaterials. Biotechnol Genet Eng Rev. Oct;33(2):144-172.

BaoLin, G., & Ma, P. X. (2014). Synthetic biodegradable functional polymers for tissue engineering: a brief review. Science China. Chemistry, 57(4), 490–500. https://doi.org/10.1007/s11426-014-5086-y

Boccaccini, A. R., & Blaker, J. J. (2005). Bioactive composite materials for tissue engineering scaffolds. Expert review of medical devices, 2(3), 303-317.

Bružauskaitė, I., Bironaitė, D., Bagdonas, E., & Bernotienė, E. (2016). Scaffolds and cells for tissue regeneration: different scaffold pore sizes-different cell effects. Cytotechnology, 68(3), 355–369. https://doi.org/10.1007/s10616-015-9895-4

von Burkersroda, F., Schedl, L., & Göpferich, A. (2002). Why degradable polymers undergo surface erosion or bulk erosion. Biomaterials, 23(21), 4221–4231. https://doi.org/10.1016/s0142-9612(02)00170-9

Callister W. D., & Rethwisch D. G. (2016). Fundamentals of Materials Science and Engineering: An integrated approach, 5th Edition. Wiley.

Casalini T. (2017). "Bioresorbability of Polymers," in Bioresorbable Polymers for Biomedical Applications: From Fundamentals to Translational Medicine (Elsevier), 65–83. 10.1016/B978-0-08-100262-9.00003-3

Chopra H, Singh I, Kumar S, Bhattacharya T, Rahman MH, Akter R, Kabir MT. (2022) A Comprehensive Review on Hydrogels. Curr Drug Deliv.19(6):658-675. doi: 10.2174/1567201818666210601155558

Ding, T., Kang, W., Li, J., Yu, L., & Ge, S. (2021). An in situ tissue engineering scaffold with growth factors combining angiogenesis and osteoimmunomodulatory functions for advanced periodontal bone regeneration. Journal of nanobiotechnology, 19(1), 247. https://doi.org/10.1186/s12951-021-00992-4

Doberenz, F., Zeng, K., Willems, C., Zhang, K., & Groth, T. (2020). Thermoresponsive polymers and their biomedical application in tissue engineering–a review. Journal of Materials Chemistry B, 8(4), 607-628.

Garg Tarun, Bilandi Ajay, Kapoor Bhawna, Kumar Sunil, Joshi Ravi (2011). Scaffold: Tissue engineering and regenerative medicine. International Research Journal of Pharmacy, , 2 (12), 37-42

Gu L., Wang N., Nusblat L., Soskind R., Roth C. and Uhrich K. (2017) "pH-responsive amphiphilic macromolecular carrier for doxorubicin delivery" Journal of Bioactive and Compatible Polymers, 32(I) 3-16

Gungor-Ozkerim PS , Inci I , Zhang YS , Khademhosseini A , Dokmeci MR . (2018) Bioinks for 3D bioprinting: an overview. Biomater Sci. May 1;6(5):915-946. doi: 10.1039/c7bm00765e. PMID: 29492503; PMCID: PMC6439477.

Ho TC, Chang CC, Chan HP, Chung TW, Shu CW, Chuang KP, Duh TH, Yang MH, Tyan YC. (2022) Hydrogels: Properties and Applications in Biomedicine. Molecules. May 2;27(9):2902. doi: 10.3390/molecules27092902.

Ikada Y. (2006) Challenges in tissue engineering. J R Soc Interface. (3):589-601.

Ji S , Dube K , Chesterman JP , Fung SL , Liaw CY , Kohn J , Guvendiren M . (2019) Polyester-based ink platform with tunable bioactivity for 3D printing of tissue engineering scaffolds. Biomater Sci. Jan 29;7(2):560-570. doi: 10.1039/c8bm01269e. PMID: 30534726; PMCID: PMC6351207.

Karanth H. and Murthy P. (2007)"pH-Sensitive liposomes—principle and application in cancer therapy" Journal of pharmacy and pharmacology, 59:469-483

Katari, R. S., Peloso, A., & Orlando, G. (2014). Tissue engineering. Advances in surgery, 48, 137–154. https://doi.org/10.1016/j.yasu.2014.05.007

Khorsandi D, Fahimipour A, Abasian P, Saber SS, Seyedi M, Ghanavati S, Ahmad A, De Stephanis AA, Taghavinezhaddilami F, Leonova A, Mohammadinejad R, Shabani M, Mazzolai B, Mattoli V, Tay FR, Makvandi P. (2021) 3D and 4D printing in dentistry and maxillofacial surgery: Printing techniques, materials, and applications. Acta Biomater. Mar 1;122:26-49. doi: 10.1016/j.actbio.2020.12.044.

Kim Y. and Matsunaga Y. (2017) "Thermo-responsive polymers and their application as smart biomaterials" Journal of Materials Chemistry B

Kirsch, M., Birnstein, L., Pepelanova, I., Handke, W., Rach, J., Seltsam, A., Scheper, T., & Lavrentieva, A. (2019). Gelatin-Methacryloyl (GelMA) Formulated with Human Platelet Lysate Supports Mesenchymal Stem Cell Proliferation and Differentiation and Enhances the Hydrogel's Mechanical Properties. Bioengineering (Basel, Switzerland), 6(3), 76. https://doi.org/10.3390/bioengineering6030076

Kocak, G., Tuncer, C. A. N. S. E. L., & Bütün, V. J. P. C. (2017). pH-Responsive polymers. Polymer Chemistry, 8(1), 144-176.

Kohane, D., Langer, R. (2008) Polymeric Biomaterials in Tissue Engineering. Pediatr Res 63, 487–491. https://doi.org/10.1203/01.pdr.0000305937.26105.e7

Kricheldorf, Hans. (2009). Simultaneous Chain-Growth and Step-Growth Polymerization-A New Route to Cyclic Polymers. Macromolecular rapid communications. 30. 1371-81.

Liu, P., Skelly, J. D., & Song, J. (2014). Three-dimensionally presented anti-fouling zwitterionic motifs sequester and enable high-efficiency delivery of therapeutic proteins. Acta biomaterialia, 10(10), 4296-4303.

Mallandrich M., Fernández-Campos F., Clares B., Halbaut L., Alonso C., Coderch L., Garduño-Ramírez M.L., Andrade B., Del Pozo A., Lane M.E., et al. (2017) Developing Transdermal Applications of Ketorolac Tromethamine Entrapped in Stimuli Sensitive Block Copolymer Hydrogels. Pharm. Res.;34:1728–1740.

Mastroianni, M., Ng, Z. Y., Goyal, R., Mallard, C., Farkash, E. A., Leonard, D. A., Albritton, A., Shanmugarajah, K., Kurtz, J. M., Sachs, D. H., Macri, L. K., Kohn, J., & Cetrulo, C. L., Jr (2018). Topical Delivery of Immunosuppression to Prolong Xenogeneic and Allogeneic Split-Thickness Skin Graft Survival. Journal of burn care & research : official publication of the American Burn Association, 39(3), 363–373. https://doi.org/10.1097/BCR.0000000000000597

Mountaki, S.A.; Kaliva, M.; Loukelis, K.; Chatzinikolaidou, M.; Vamvakaki, M. (2021) Responsive Polyesters with Alkene and Carboxylic Acid Side-Groups for Tissue Engineering Applications. Polymers, 13, 1636.

Moysidou C-M, Barberio C and Owens RM (2021) Advances in Engineering Human Tissue Models. *Front. Bioeng. Biotechnol.* 8:620962

Osborn, T. M., Hallett, P. J., Schumacher, J. M., & Isacson, O. (2020). Advantages and Recent Developments of Autologous Cell Therapy for Parkinson's Disease Patients. Frontiers in cellular neuroscience, 14, 58. https://doi.org/10.3389/fncel.2020.00058

Park H, Guo X, Temenoff JS, Tabata Y, Caplan AI, Kasper FK, Mikos AG (2009). Effect of swelling ratio of injectable hydrogel composites on chondrogenic differentiation of encapsulated rabbit marrow mesenchymal stem cells in vitro. Biomacromolecules;10(3):541-6. doi: 10.1021/bm801197m.

Parkatzidis K, Chatzinikolaidou M, Kaliva M, Bakopoulou A, Farsari M, Vamvakaki M. (2019) Multiphoton 3D Printing of Biopolymer-Based Hydrogels. ACS Biomater Sci Eng.;5(11):6161-6170.

Pepelanova, I., Kruppa, K., Scheper, T., & Lavrentieva, A. (2018). Gelatin-Methacryloyl (GelMA) Hydrogels with Defined Degree of Functionalization as a Versatile Toolkit for 3D Cell

Culture and Extrusion Bioprinting. Bioengineering (Basel, Switzerland), 5(3), 55. https://doi.org/10.3390/bioengineering5030055

Read-Fuller, A. M., Yates, D. M., Radwan, A., Schrodt, A. M., & Finn, R. A. (2018). The Use of Allogeneic Cartilage for Grafting in Functional and Reconstructive Rhinoplasty. Journal of oral and maxillofacial surgery : official journal of the American Association of Oral and Maxillofacial Surgeons, 76(7), 1560.e1–1560.e7. https://doi.org/10.1016/j.joms.2018.03.021

Reddy MSB, Ponnamma D, Choudhary R, Sadasivuni KK (2021). A Comparative Review of Natural and Synthetic Biopolymer Composite Scaffolds. Polymers (Basel). Mar 30;13(7):1105. doi: 10.3390/polym13071105.

Reid, B., Gibson, M., Singh, A., Taube, J., Furlong, C., Murcia, M., & Elisseeff, J. (2015). PEG hydrogel degradation and the role of the surrounding tissue environment. Journal of tissue engineering and regenerative medicine, 9(3), 315–318. https://doi.org/10.1002/term.1688

Reusch W., Textbook of Organic Chemistry, Wiley, 2010

Sávio-Silva, C., Beyerstedt, S., Soinski-Sousa, P. E., Casaro, E. B., Balby-Rocha, M. T. A., Simplício-Filho, A., Alves-Silva, J., & Rangel, É. B. (2020). Mesenchymal Stem Cell Therapy for Diabetic Kidney Disease: A Review of the Studies Using Syngeneic, Autologous, Allogeneic, and Xenogeneic Cells. Stem cells international, 2020, 8833725. https://doi.org/10.1155/2020/8833725

Schmaljohann D. (2006) “Thermo- and pH-responsive polymers in drug delivery” Advanced Drug Delivery Review, 58 , 1655–1670.

Schmalz, G., & Galler, K. M. (2017). Biocompatibility of biomaterials–Lessons learned and considerations for the design of novel materials. Dental Materials, 33(4), 382-393.

Sénéchal, V., Saadaoui, H., Rodriguez-Hernandez, J., & Drummond, C. (2017). Electro-responsive polyelectrolyte-coated surfaces. Faraday discussions, 199, 335–347. https://doi.org/10.1039/c6fd00246c

Sharifi, S., Sharifi, H., Akbari, A., & Chodosh, J. (2021). Systematic optimization of visible light-induced crosslinking conditions of gelatin methacryloyl (GelMA). Scientific reports, 11(1), 23276. https://doi.org/10.1038/s41598-021-02830-x

Sindhu, K. R., Bansode, N., Rémy, M., Morel, C., Bareille, R., Hagedorn, M., Hinz, B., Barthélémy, P., Chassande, O., & Boiziau, C. (2020). New injectable self-assembled hydrogels that promote angiogenesis through a bioactive degradation product. Acta biomaterialia, 115, 197–209. https://doi.org/10.1016/j.actbio.2020.08.012

Stoychev, G., Kirillova, A., & Ionov, L. (2019). Light-responsive shape-changing polymers. Advanced Optical Materials, 7(16), 1900067.

Sun, Xiaohang & Agate, Sachin & Salem, Khandoker & Lucia, Lucian & Pal, Lokendra. (2020). Hydrogel-Based Sensor Networks: Compositions, Properties, and Applications - A Review. ACS Applied Bio Materials. 10.1021/acsabm.0c01011.

Vignolini, S., & Bruns, N. (2018). Bioinspiration Across All Length Scales of Materials. Advanced materials (Deerfield Beach, Fla.), 30(19), e1801687. https://doi.org/10.1002/adma.201801687

Wang, Z., Kumar, H., Tian, Z., Jin, X., Holzman, J. F., Menard, F., & Kim, K. (2018). Visible Light Photoinitiation of Cell-Adhesive Gelatin Methacryloyl Hydrogels for Stereolithography 3D Bioprinting. ACS applied materials & interfaces, 10(32), 26859–26869. https://doi.org/10.1021/acsami.8b06607

Wei M., GaoY., Li X. and Serpe M. (2017) "Stimuli-responsive polymers and their applications" Royal Society of Chemistry, Polymer Chemistry, 8, 127-143

Xu, Z. L., & Huang, X. J. (2021). Optimizing allogeneic grafts in hematopoietic stem cell transplantation. Stem cells translational medicine, 10 Suppl 2(Suppl 2), S41–S47. https://doi.org/10.1002/sctm.20-0481

Yan, Y., & Siegwart, D.J. (2014). Scalable synthesis and derivation of functional polyesters bearing ene and epoxide side chains. *Polymer Chemistry, 5*, 1362-1371.

Zhu, M., Wang, Y., Ferracci, G., Zheng, J., Cho, N. J., & Lee, B. H. (2019). Gelatin methacryloyl and its hydrogels with an exceptional degree of controllability and batch-to-batch consistency. Scientific reports, 9(1), 6863. https://doi.org/10.1038/s41598-019-42186-x